Faculteit Industriële Ingenieurswetenschappen

master in de industriële wetenschappen: chemie

Masterthesis

The optimization of the durability of returnable glass bottles after repeatedly filling

Marthe Bielen

Scriptie ingediend tot het behalen van de graad van master in de industriële wetenschappen: chemie

PROMOTOR :
Prof. dr. ir. Mieke BUNTINX

PROMOTOR :
Ing. Jonas VANDECRUYS

Gezamenlijke opleiding UHasselt en KU Leuven

Universiteit Hasselt | Campus Diepenbeek | Faculteit Industriële Ingenieurswetenschappen | Agoralaan Gebouw H - Gebouw B | BE 3590 Diepenbeek

Universiteit Hasselt | Campus Diepenbeek | Agoralaan Gebouw D | BE 3590 Diepenbeek
Universiteit Hasselt | Campus Hasselt | Martelarenlaan 42 | BE 3500 Hasselt

2022
2023

Faculteit Industriële Ingenieurswetenschappen

master in de industriële wetenschappen: chemie

Masterthesis

The optimization of the durability of returnable glass bottles after repeatedly filling

Marthe Bielen

Scriptie ingediend tot het behalen van de graad van master in de industriële wetenschappen: chemie

PROMOTOR :

Prof. dr. ir. Mieke BUNTINX

PROMOTOR :

Ing. Jonas VANDECRUYS

UHASSELT KU LEUVEN

Acknowledgements

I would like to express my deepest appreciation to Ing. Jonas Vandecruys to allow me to conduct my master's thesis at AB InBev, despite the late application, and offering me an educational and unique research objective. I am grateful for the independence he offered me and how he was always ready to offer help. He was always supportive of my ideas and added new ideas himself to complete the study in the best way possible. I could not have undertaken this journey without Prof. dr. ir. Mieke Buntinx. I benefited greatly from the constructive feedback she offered me. I would like to thank her for her positivity which motivated me tremendously. I would like to extend my sincere thanks to Karolien Vervloet and Marleen Bleyen, the glass team at GPDIL, for their support during this study. I would like to thank them for their help and explanation in teaching me how to work with the used devices and for the several new skills they taught me. Lastly, I'd like to acknowledge Geert Vanham for the time he spent preparing the scuffing simulator.

Table of contents

List of Tables

List of Figures

List of abbreviations

B2B	Business-to-business
B2C	Business-to-consumer
CC	Climate change
CE	Circular economy
CPS	cm/s
DoE	Design of Experiments
EMF	Ellen Macarthur Foundation
FRDP	Fossil resource depletion potential
GHG	Greenhouse gas
GITEC	Global Innovation and Technology Centre
GPDIL	Global Packaging and Dispense Innovation Laboratory
GTS	General Technical Specifications
GWP	Global warming potential
IPR	Internal pressure resistance
LCA	Life cycle analysis
OOS	Out-of-specification
PET	Polyethylene terephthalate
RB	Refillable bottles
RPM	Revolutions per minute
RPT 2	Ramp Pressure Tester 2
SB	Single-use bottles
VLT	Vertical Load Tester

Abstract

Driven by sustainability, AB InBev, the world's largest brewery aims to stimulate the use of circular packaging. Refillable glass bottles are collected after use, sterilized, and refilled before they are put back on the market. To analyse whether the strength of refillable bottles is sufficient for multiple cycles, insight into the internal pressure, top load pressure, impact, and friction resistance based on simulation testing is required. The internal pressure resistance (IPR) measured by applying a hydrostatic pressure is chosen as a reference value for the strength of the bottle. After applying topload pressure, impact, or friction, the IPR is determined and compared with the reference. In addition, combinations are applied to the bottles to investigate possible interactions between the three factors. This study shows that all tested bottles meet the standards set for refillable bottles for all individually applied factors. The analysis reveals that friction, from the moment it causes scuffing, has the greatest effect on the bottle's strength and thereby causes a significant decrease in the measured IPR. Next to friction, impact also causes a significant difference in measured IPR values. Internal pressure and topload pressure do not affect strength in the tested conditions. Finally, combinations of friction, impact, and/or topload pressure show that there are no interactions between the three factors. In conclusion, test simulations to evaluate the quality of refillable bottles should surely involve friction and impact.

Samenvatting

Omdat duurzaamheid een belangrijke drijfveer is voor AB InBev, ’s werelds grootste brouwerij, wordt het gebruik van circulaire verpakking sterk gestimuleerd. Hervulbare flessen worden na gebruik verzameld, gesteriliseerd en opnieuw gevuld voordat ze weer op de markt worden gebracht. Om te analyseren of de sterkte van hervulbare flessen voldoende is voor meerdere cycli, is inzicht nodig in de interne druk, topbelasting, impact en wrijving op basis van simulatietesten. De interne drukweerstand (IPR) op basis van hydrostatische druk wordt gekozen als referentiewaarde voor de sterkte van de fles. Na het toepassen van topload druk, impact of wrijving wordt de IPR opnieuw bepaald en vergeleken met de referentie. Vervolgens worden combinaties toegepast om eventuele interacties tussen de drie factoren te analyseren. De studie toont aan dat de geteste flessen voor alle individueel toegepaste factoren voldoen aan de normen voor hervulbare flessen. Uit de analyse blijkt dat wrijving, vanaf het moment dat het zichtbare schade veroorzaakt, het grootste effect heeft op de sterkte van de fles en daarmee zorgt voor een significante afname van de IPR. Naast wrijving veroorzaakt impact ook een significante daling in IPR-waarden. Interne druk en topbelasting hebben in de geteste condities geen effect op de sterkte. Toepassing van combinaties van wrijving, impact en/of toploaddruk onthullen geen interacties tussen de drie factoren. Testsimulaties om de kwaliteit van hervulbare flessen te evalueren moeten dus zeker wrijving en impact omvatten.

1. Introduction

1.1 Context

Anheuser-Busch InBev, also known as AB InBev, is by far the largest brewery in the world. The headquarters of this multinational is located in Leuven, Belgium. AB InBev mainly produces brands such as Stella Artois, Budweiser, and Corona, as well as some local specialties. In Belgium, these include brands such as Jupiler, Hoegaarden, Leffe, and Tripel Karmeliet [1].

It is widely known that most beer brands have their own bottle that distinguishes them from others to promote sales and make clear to consumers which brand they are drinking. This can be done through both the label and crown cap on the bottle and the shape and colour of the bottle itself. In this research, a distinction is made between two different types of returnable bottles: A and B (Figure 1). Both of these bottles have a specific height, diameter, and thickness in addition to their unique shape and colour.

A *B*

Figure 1: Appearance of returnable glass bottles A and B [2]

Since sustainability is an important driver for AB InBev, the company is strongly committed to circular packaging (see paragraph 2.2). The Global Innovation and Technology Centre, also known as GITEC, is working on the design of packaging that consists of as much recycled material as possible. They also try to reduce the amount of material used in their packaging. GITEC developed the world's lightest beer bottle which weighs only 150 g compared to the usual 180 g [3] [4].

In the Global Packaging and Dispense Innovation Laboratory (GPDIL) at AB InBev, the various packaging types for beer designed by GITEC, are validated and tested for quality. For beer packaging, the commonly used materials include glass, metal, and plastics, but coatings, labels, and crown caps are also analysed in the lab.

When it comes to glass bottles specifically, a distinction is made between one-way bottles, returnable bottles, and reusable or refillable bottles. To work towards their circular packaging goals (see paragraph 2.2), AB InBev has developed projects to increase the collection efficiency of used bottles. Collected bottles can be refilled after a washing process. Most of the refillable bottles can be used up to fifteen times, while some can even be used up to one hundred times. Approximately 35% of the volume of beer is sold in returnable packaging such as refillable glass bottles, which are nearly five times less carbon-intensive when compared to one-way bottles [5]. However, disposable bottles can still be recycled, leaving the glass in circulation.

1.2 Problem definition

Since reusing glass bottles is important to ensure circular packaging of the beer, these bottles must therefore meet certain quality requirements. According to the standard for reuse of packaging ISO 18603:2013 [6], the bottles need to be cleaned before they can be reused and they must not have suffered excessive visual damage. In addition, the strength of the bottles must be sufficiently higher than the one-way bottles, because the refillable bottles will travel a path where the risk of damaging the glass is real. The bottles are transported and carried on a conveyer belt for multiple cycles, and come in contact with other bottles and other materials that can have an impact on the bottles, etc. The main factors that affect the strength of glass bottles during repeated filling are internal pressure, topload pressure, impact, and friction.

Bottles that are not collected and those that are collected, but do not meet the quality requirements are lost. A certain proportion of refillable bottles cannot be reused because they break in the chain. This can happen either at the producer, the retailer, the consumer, or during transportation. During the washing, filling, and packing steps at AB InBev, bottles are most likely to break during the pasteurization, as a result of pressure and temperature. The broken bottles at this location can be removed relatively easily without having to stop the line to do so. In addition, splitting the line at certain places during these steps allows the process to keep running at all times. Thus, one line will always still be working while another needs to be shut down for the removal of broken bottles or maintenance.

Bottle breakage creates more glass waste that can be recycled. However, recent life cycle analysis (LCA) studies indicate that recycling has a greater negative impact on the planet than reuse. It has been shown that the impact of the collection and refilling of returnable bottles is effectively smaller after just one refill [7]. As a consequence, if the bottles that are meant to be reused break too often, AB InBev will not be able to obtain the predetermined goals.

By counting the number of new bottles, produced from raw or in the best case recycled materials, that need to be replenished to complete the pool, the number of returnable bottles that are effectively rebottled, for which they are designed, can be estimated. This number strongly depends on the type of bottle and the market they end up in. To ensure the desired durability, the company aims to bring 100% reusable packaging or packaging made up mostly of recycled material to the market by 2025 [8].

1.3 Research objectives

To ensure that the bottles produced for refill meet the set requirements needed for reuse, they must undergo testing in the lab that simulates potential worst-case scenarios. The simulation should be a quick and user-friendly method and must include the most common factors that can cause damage to a bottle, being: i) friction, ii) pressure, and iii) impact. One must also be aware of the effects the three individual factors can have on each other and whether the order in which they are applied affects the strength of the glass bottles.

The main objective of this study is to quantify the relationship between the individual and combined effects of friction, pressure, and impact on the strength of selected types of glass bottles to predict the quality of reusability in a simulation process.

First, different simulation methods, devices, and settings to exert friction, pressure, and impact on the bottles, both individually and combined, must be mapped out. The simulation will be considered

acceptable if the bottles that survive the simulation can withstand the actual process of sterilization and refilling for several cycles without breaking.

Second, it is important to have a comprehensive knowledge of the fractography of glass and what factors affect how the glass will break to find out where the origin of the fracture is located and to quantify how much stress in the bottle caused the breakage.

Then, the conditions under which a bottle breaks are determined. Based on the knowledge of fractography, the individual effects of friction, pressure, and impact on the strength and possibly the breakage of glass are quantified. This way, the amount of stress and tension a bottle can resist can be analysed and compared. Through a Design of Experiments (DoE), the combination of the three factors can be analysed to find a relationship between them. Based on this correlation, the tests that must be performed to subject a glass bottle to the best possible simulation of the reusing process can be identified.

Finally, one can distinguish between different types of glass bottles. For example, each brand provides a different shape, volume, thickness, and colour of glass bottles.

1.4 Preview

The next chapter two describes preliminary research on the circular economy in which packaging, including glass bottles, is reused in the original form. More information is shared about the company AB InBev and its vision of sustainability. Finally, the importance of glass bottles and the way glass breaks under different loads are discussed.

Chapter three gives a description of the materials and the approach, in which the operation of various devices and test methods are explained.

The different results are described and analysed in chapter four. Some of the test methods were first optimized in order to continue with the most accurate method. During the testing of the individual effects, the influence of different settings was also examined. For each factor, the size of the effect on the strength of the bottles was examined. Finally, combinations of the three factors were applied to determine the interactions between the effects.

Finally, the conclusion of this study is written down in chapter five.

2. Preliminary research on the durability of returnable glass bottles

2.1 Circular economy

Circular economy (CE) refers to a sustainable model that replaces the linear take-make-waste system by seeking to close material cycles in terms of biology and technology. This model reduces waste by focusing on keeping the value of resources and materials as much and as long as possible within the economy. Besides the elimination of waste and the circulation of materials, the regeneration of nature is the third principle on which the CE is based. Global challenges such as climate change (CC), biodiversity loss, waste, and pollution are tackled by the CE model [9].

The second principle of the CE is the continuous circulation of materials as shown in the CE diagram, also known as the butterfly diagram (Figure 2), consisting of a biological cycle and a technical cycle. To regenerate nature, the biological cycle makes sure all nutrients from biodegradable materials are returned to Earth. In the technical cycle, materials are kept in circulation through different processes, such as recycling, remanufacturing, repairing, and reusing [10].

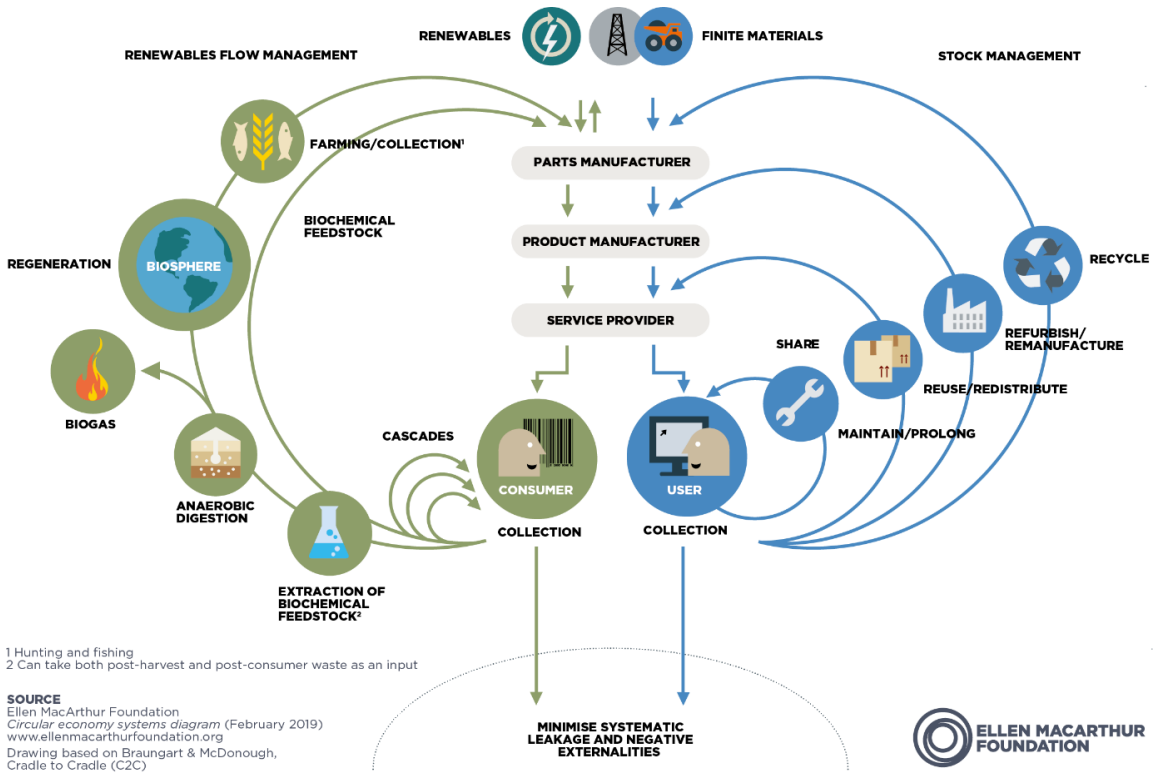

Figure 2: Circular economy butterfly diagram [11]

To keep the packaging in circulation at a high value, different businesses have introduced reusable packaging. Reusable packaging plays a key role in the reduction of packaging waste and offers several business benefits, such as better customer relationships and lower costs. Based on whether the reusable packaging is refilled by the user or returned to the company and whether this refill or return could be done at home or on the go, four different reuse models can be distinguished (Figure 3) [12].

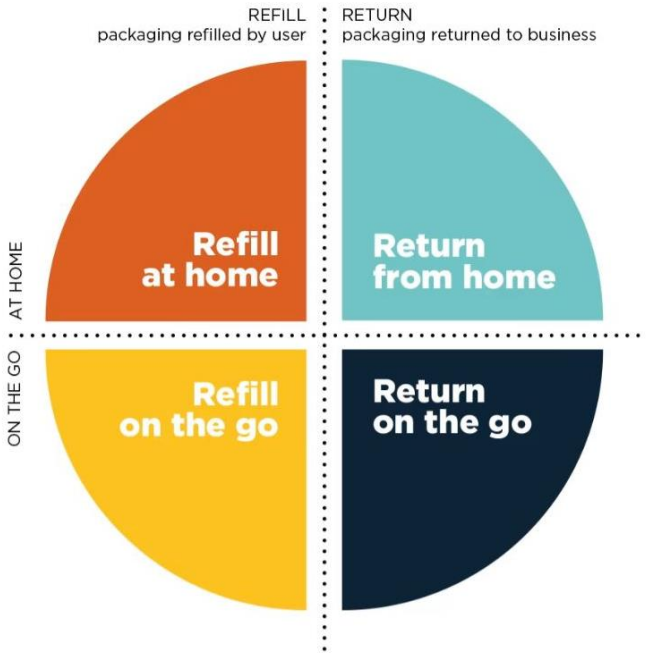

Figure 3: Four business-to-consumer reuse models [12]

The ultimate goal of CE is to minimize the harmful environmental impacts of the resulting material cycle purchases by dematerializing our economy. Any development of a new product, process, or building must consider the full life cycle of the product. The product must be produced in a way that it will be easily reused or recycled while using as little material as possible [13].

The Ellen Macarthur Foundation (EMF) is a non-profit organisation that works as a registered charity committed to creating a CE. The organisation conducts research on the implementation of the three CE principles into practice and the benefits that result. The EMF works together with international institutions, governments, universities, and many others to promote the idea of a CE by supporting organisations and individuals with formal learning opportunities. By creating resources, publications, and tools they help ensure effective policies and create better designs to create circular products [14].

2.2 AB InBev's vision to contribute to a circular economy

As the world is facing a scarcity of resources, AB InBev is not lagging in contributing its share to the CE, in terms of agriculture, water use, and packaging. Since 36.4% of their greenhouse gas (GHG) emissions come from packaging alone, they take a circular approach to packaging by increasing the amount of recycled material in their packaging and reusing their packaging to reduce waste. AB InBev has set a target to achieve by 2025 to provide their business with long-term financial benefits and packaging supply security. To achieve this goal, they must ensure that 100% of the beer they sell is packed in packaging that consists mainly of recycled material or packaging that is returnable. Returnable glass bottles and returnable kegs should replace the single-use alternative to reduce the need for virgin material and GHG emissions (Figure 4). Packaging types that are not returnable, such as aluminium cans and polyethylene terephthalate (PET) bottles should reach a minimum of 50% recycled content. This goal applies mainly to the primary packaging which represents 85% of the total packaging volume by weight, but includes secondary packaging and post-consumer waste [5].

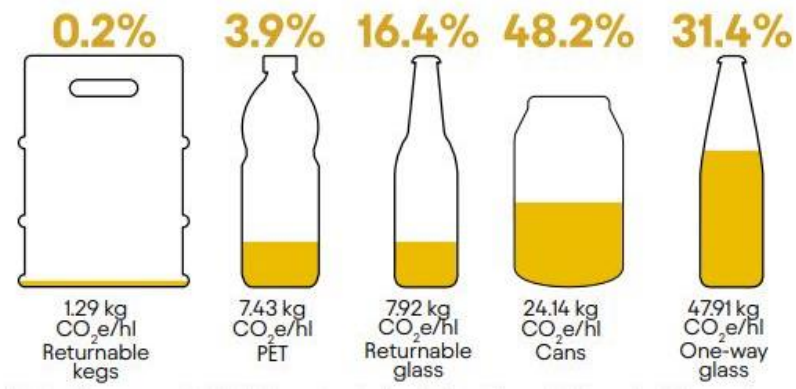

Figure 4: Greenhouse gas emissions by packaging type [15]

To guarantee the long-term security of the supply of packaging they promote the recovery and reuse of packaging in its original form. The company believes that offering sustainable solutions, such as returning packaging to the market, will help consumers understand the value of the CE and lead to more sustainable consumer behaviour.

To this day, approximately 35% of the beer sold by AB InBev is already packed in returnable glass bottles. AB InBev's innovation team at the Global Innovation and Technology Centre (GITEC) focuses on promoting the recovery of all returnable bottles and reusing the packaging in its original form. The returnable bottles are, according to AB InBev, almost five times less carbon-intensive than disposable bottles. This is because most reusable bottles can be refilled and sold up to 15 times [5].

The first method for the recovery of the returnable bottles takes place whenever customers buy beer bottles from supermarkets or liquor stores to drink at home. They then return the empty bottles to the place of purchase. This 'return-on-the-go' approach [12] is one of four business-to-consumer (B2C) reuse models (Figure 5).

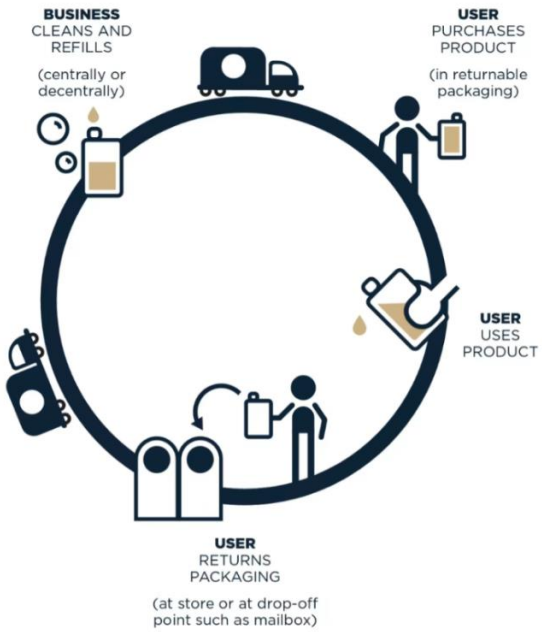

Figure 5: 'Return on the go' reuse model [12]

The supermarket or liquor store serves as a third-party business and is not responsible for the reusable packaging or the handling of the washing and refilling steps. Once the supermarket or liquor store has collected the empty beer bottles from the customers, AB InBev will collect, clean and refill the bottles and redeliver the filled bottles to the supermarkets and liquor stores. Bars and restaurants also use this business-to-business (B2B) system, which is similar to the B2C 'return from home' reuse model (Figure 6) [12].

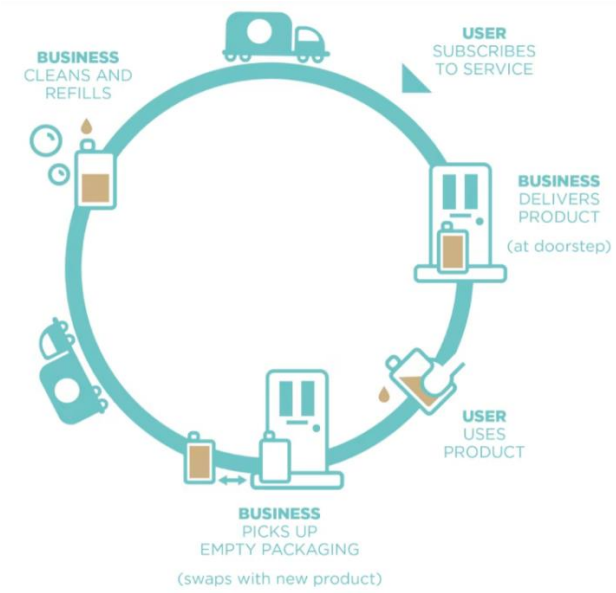

Figure 6: 'Return from home' reuse model [12]

2.3 Glass bottles

This study will focus on the optimization of the durability of returnable glass bottles. As shown in Figure 4, returnable glass bottles are a preferable type of beer packaging over aluminium cans in terms of GHG emissions. Returnable glass bottles are washed and refilled for a dozen of cycles, while aluminium cans can only be used once before becoming waste. Besides the smaller amount of emissions, beer stored in glass bottles tends to maintain its cold temperature for longer compared to beer packed in aluminium cans.

Plastic bottles seem to have lower emissions than glass bottles (Figure 4), although plastic is not often used as packaging for beer. This is a result of the inferior oxidation prevention and carbonation retention of plastic bottles. In addition, plastic does not provide good protection from heat and sunlight, so the beer goes stale faster [16].

Besides the possibility to return glass bottles, there are many other reasons why beer is best packed in glass packaging. The first reason is the unique and traditional experience of drinking beer out of a glass bottle. To protect the beer from external influences, it is important to choose the right type of packaging. Glass forms an effective barrier against the loss of aromas and contact with oxygen since the oxidation of beer can cause the beer to become stale. Glass does not harm ocean or marine life with toxic materials as a result of being made out of all-natural ingredients such as sand. Consisting of only one type of material also facilitates the recycling process of glass. Glass bottles are easily and endlessly recyclable into new bottles or any other food containers. The quality of the glass packaging will remain the same, even after being recycled. In addition, the unique design of a glass bottle, with a variety of shapes and colours, ensures the recognizability of the beer and the brand [16].

2.4 Returnable glass bottles

2.4.1 Sustainability

To reduce the environmental impact of glass beverage bottles, reusing them could be a sustainable solution. Reuse allows the bottle to be recovered in its entirety to avoid the need for virgin glass. Life Cycle Assessments (LCA) include a life-cycle perspective of products from the purchase of the raw materials to the disposal at the end-of-life, following the principles and guidelines of ISO 14040:2006 and ISO 14044:2006. The internal recycling and reuse of glass bottles, the minimization of waste, and many other sustainable production concepts can be analysed based on LCA. LCA studies can help companies to identify and reduce certain environmental impacts and resulting liability, and save a considerable amount of time and money [17].

LCA is used to compare the impact on the environment of reusable and non-returnable glass bottles as packaging for liquids, to decide whether a reusable system is advantageous based on the outcome. The energy needs of a one-way beer bottle take the following aspects into account: the production of the glass, the production of the secondary and tertiary packaging, and the transportation of the bottles to the distributor. Many more energy-consuming steps are involved whenever bottles are being collected and reused. Returned post-consumer bottles need a washing step, more transportation, replacement by new bottles if necessary, and transportation and recycling of the bottles that are removed from the refillable system [18]. The parts of the process that have the biggest impact on the environment are the sterilization and drying of refillable bottles. However, the impact of refillable bottles can only be compared to one-way bottles when the number of cycles is known. The impact can be reduced by 40% after reusing the glass bottle only once. After the second cycle, the benefit of reuse will not be as significant. The stabilisation of the benefit is achieved after the eighth cycle. The remarkably low savings rate is due to the increasing transport and washing impacts. The optimal number of cycles that the bottles are reused depends on the cost-effectiveness of the process [7].

Research shows that the single-use impact of a reusable bottle that was used eight times, and has therefore gone through the process of sterilization, filling, and packaging seven times, is smaller than the impact of a non-reusable bottle. This is mainly due to dividing the impact of the entire process by the number of cycles, which also divides the production and disposal of the bottle by eight, while these steps only occurred once. The ‘reuse’ process has a significant impact, because of the washing and the transportation to the collection centre and the companies [7].

The steps of a refillable process can be divided into three stages: production and end-of-life, reconditioning, and distribution. The contribution of these stages is depending on the number of refills. During the reconditioning of the refillable bottles, the first washing and the bottling take place. The main burdens during these steps are the electricity consumption, the replacement of the caps in the generated bottles, the heating of the washing water, and the water consumption. The transportation to the local distributor, for which the distance is considered 200 km, forms the biggest impact during the distribution stage. In the evaluation of the impact, distance plays an important role. The increase in distance between the bottling plant and the local distributor ensures that the number of refills must increase to keep the environmental impact the same [19]. A reduction in the average distance of transportation improves the overall performance of the heavier packages compared to the lighter ones [20]. The contribution of the reconditioning and the distribution increases with the number of refills.

Figure 7 shows the ratio of the factor climate change (CC) between the refillable bottle (RB) system and the single-use bottle (SB) system, with N the number of refills for the RB. If the RB would only be refilled once, the SB would be the preferable option in terms of impact on CC. Since the impact of the

RB is in this case bigger than the impact of the SB, the ratio measures over 100%. The use of an RB system already becomes the more interesting option after only two refills (N = 2) as this system has a significantly smaller impact on CC as a result of two refills. After two refills, the ratio between the RB system and the SB system ranges from 44% to 74% depending on other indicators. This ratio decreases as the number of refills N increases according to an Italian study [19].

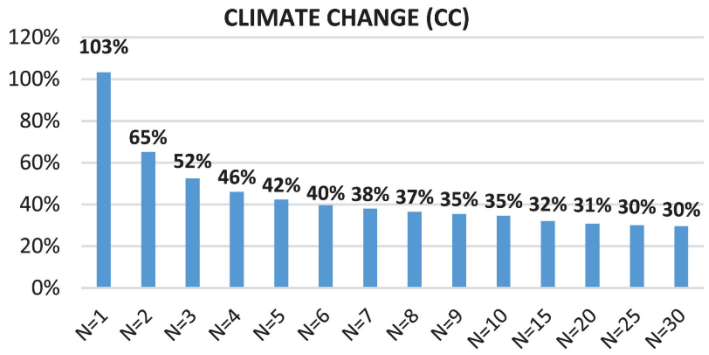

Figure 7: Ratio between the value of climate change in the RBs and the SBs system [19]

A study has been done on the types of packaging of seven microbreweries. The replacement of single-use packaging with refillable glass bottles or aluminium cans provides a reduction in global warming potential (GWP) burdens. Depending on the brewery and thus the distance to the distributor, one of the two packaging alternatives will provide a greater GWP reduction. This reduction can be broken down into four relevant stages of the life cycle of beer packaging. The results for refillable glass bottles are an increase of 4% in upstream transport burdens and an increase of 3% in downstream transport burdens, due to the slight increase in weight of the bottles compared to single-use bottles to obtain a glass bottle that can last several cycles. However, a reduction of 68% in packaging production burden and a 40% reduction in waste management burden are achieved by collecting and refilling the same bottles for multiple cycles. This results in an overall reduction of 13% in footprint. In addition to GWP, other impacts can also be considered. Looking at the fossil resource depletion potential (FRDP) burdens, the average upstream and downstream burdens remain the same, but packaging and waste management burdens are reduced by 64% each. The average overall footprint will result in an 11% reduction. The increase of upstream and downstream acidification burdens stays at 4% and 3% for refillable glass bottles. The overall reduction of 15% in acidification burdens is due to a reduction of 78% in packaging and a reduction of 46% in waste management. To increase the percentage of burden reduction for freshwater eutrophication, abiotic resource depletion potential, and ionizing radiation, switching to refillable bottles is the best option [21].

For refillable glass bottles, it is assumed that only the glass is reused in each refill cycle. All the other components of the packaging system or to be considered every time for each use [22]. The secondary and tertiary packaging is depending on the type of beverage being packaged and the company responsible for the packaging. The company is in control of the relative impact of the secondary and tertiary packaging compared to the glass itself. The significance of this relative impact within the life cycles is greatest for bottles of wine, according to Cleary's study on glass wine bottles. He claims that secondary and tertiary packaging is responsible for greater emissions than the emissions caused by the production of refillable glass bottles since these are divided by the number of refills. For glass wine bottles, focusing on reducing secondary and tertiary packaging and increasing the number of refills will reduce the impact of the refillable system most strongly [19].

2.4.2 Quality and safety requirements

For glass beer bottles to be refilled, they must comply with all regulations and laws regarding food safety in both the country of production and the county where the product will be marketed. The bottles must be safe for use in contact with beverages and should be free of contaminants [23]. The washing of the bottles must be done in such a way that no residue remains, but certainly, no pathogens or other microorganisms could get into the beer. The bottles must be as clean as they were before the very first filling. This study will not elaborate further on the safety rules associated with the cleaning and refilling of glass bottles.

Besides the safety rules, there are quality rules that refillable bottles must comply with in order to be allowed to be re-marketed after refilling. The visual damage that a glass bottle has incurred during production up to the filling, packing, transport, and usage must be limited. Finally, the strength of refillable bottles used for carbonated beverages must meet the quality requirements aggregated by AB InBev in the Global Packaging General Technical Specifications (GTS) [23] in terms of internal pressure, topload pressure, and impact, among others, for them to store beverages at elevated pressure after repeated filling. AB InBev's internal quality requirements are similar to source documents DT 14.01 and DT 14.10 [24]. The strength of the bottle must be guaranteed to reduce the chance of a safety hazard as a result of a lower failure pressure. If the pressure occurring inside the bottle, due to the carbonation of the beverage, is not sufficiently lower than the pressure that the bottle can resist, the bottle may explode with low-pressure impacts [25]. The quality requirements will also be used to determine the usable life of returnable glass bottles in this study.

2.5 Glass

2.5.1 Strength

Glass by nature is a very strong material with a theoretical strength of 25-30 GPa. The strength of glass shows its resistance to fracture when exposed to external loads. The ability to resist fracture is the limit of strength minus the maximum stress which causes the destruction of the material under a static load.

The high natural strength of glass as a result of the structure of the material hardly occurs in practice. The strength of the tested glass sample is directly determined by the state of the surface of the samples. Depending on the superficial and the internal cracks in the sample of glass the strength will differ from the natural strength. Cracks and other imperfections occurring on the surface, such as scratches and inclusions, concentrate the stress. The formation of imperfections in the glass, and the reasons for the decrease in strength are a result of the different parameters of the process, the cutting, the storage, the transportation, and the environmental effects [26]. Imperfections that are formed naturally during the fabrication process and cannot be avoided are considered intrinsic. Extrinsic origins, on the other hand, are formed in the steps that follow the fabrication and are a result of machining, handling, impact, wear, oxidation, or corrosion [27]. Cracks are mostly formed during the forming and annealing of glass. During the formation of glass, the outer surface layer will start to solidify, while the rest of the volume stays in the plastic state. Due to the thermal expansion of the material in the volume, micro-cracks will form on the surface [26].

Imperfections that occur at the surface of a glass bottle can reduce the required pressure to fail significantly. The size of these imperfections plays a key role in the determination of failure stress, unlike the shape and location of the flaw. For the bottles in which the fracture origin is located at an imperfection, the initial crack forms in the direction of the bottle axis. Crack branching orientated along

the bottle axis is a result of the most energy being released whenever a crack propagates perpendicular to the stress [25].

The share of the influence of the environment on the strength of glass depends on several factors such as the contact time and the temperature. The duration and the magnitude of the stress appearing in the sample also affect the strength. High-humidity environments cause a significant decrease in strength levels, as a result of the lengthening of the cracks already existing and the emergence of new micro-cracks.

2.5.2 Breakage

The breakage of a glass sample is a quite complex process. The development of this process is depending on different parameters such as the structure of the material, the parameters of the defects, the stress state of the sample, the loading rate, etc. The kinetics of a fracture can be divided into stages. First, micro-cracks will grow at an accelerating speed. At the moment the stress at the tip of one of the micro-cracks reaches the theoretical strength, the crack will lengthen causing the sample to break completely at a constant high speed [26].

The patterns of a general crack extension point back to the origin of the fracture, the flaw from which cracking begins. A crack propagates perpendicular toward the point where the local principal tension stress is greatest. A crack can fork or branch into multiple propagating cracks according to the law of normal crack propagation.

The fracture origin is in most cases the part of the glass that had the worst combination of stress and flaw severity. Besides, information about the cause of the fracture, the energy of the fracture, and the state and magnitude of stress are provided by the breakage pattern. Often, the reassembly of the specimen is needed for the examination and the finding of the origin. Figure 8 shows the region where the two pieces with the origin join across a flat surface, which can be found by studying the branching patterns and tracing them back to the origin [27].

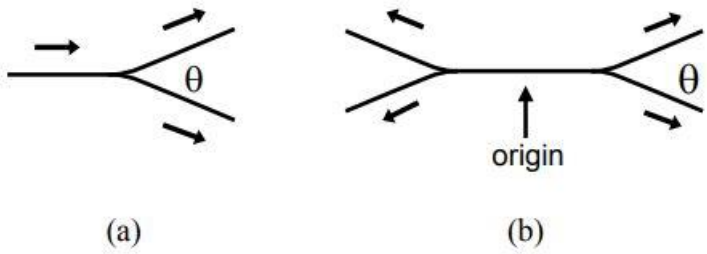

Figure 8: Crack branching indicates the direction of crack propagation [27]

The amount of branching that occurs is dependent on the failure stresses. Branching may not occur at all whenever the failure stresses are low. The higher the stresses, the higher the energy available for causing a fracture. High-energy fractures create maximal branching and therefore a high number of small fragments. The angle between two cracks developed from a single crack varies with the stress state. A propagating crack travels a certain distance before branching which is related to the stresses and the stored energy in the specimen [27].

2.5.3 Fractography

Fractography involves the analysis of fracture surfaces, including glass, to identify the fracture origins. The examination of the fracture surface of broken components of glass enables the characterization of the fracture cause. The examination contains the analysis of the size, shape, and breakage patterns of the fragments, following the standard for fractography ASTM 1322 to determine whether a fracture was thermally driven or mechanically driven, whether the stress was large or small, and whether the stresses were uniaxial or multiaxial. Hackle lines, haze, and mirrors (Figure 9) are patterns that can be recognised and tell something about the specific fracture [27].

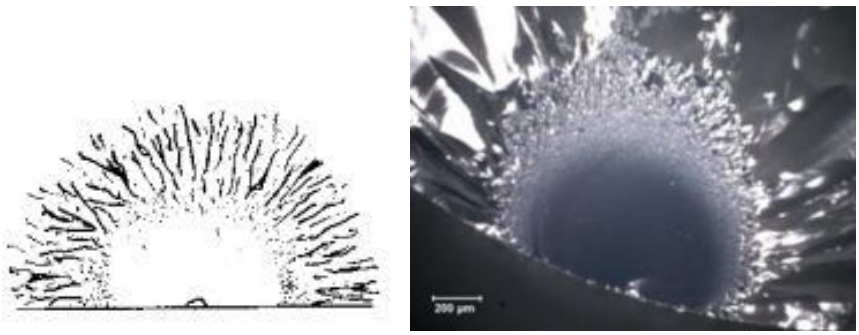

Figure 9: Fracture mirror [27]

To identify the imperfections in the glass that may cause a reduction in strength, the glass sample will be intentionally fractured in the laboratory. This way the cause of breakage is known, which simplifies the fractographic analysis. To smooth the process specimens should be marked with indications of orientation or specific locations [27].

2.6 Testing methods to simulate and analyse

For refillable bottles to comply with all quality requirements, they must be able to withstand several loads that will occur during their life cycle, being internal pressure, topload pressure, impact, and friction. The bottles will be tested for these types of loads in lab conditions using different methods (see chapter 3). Before these loads can be applied to the bottles, it is important to have a better understanding of the effect the different loads will have on the bottles and how the bottle will behave during the application of these loads. With this information, the cause of a particular fracture can be recognised based on the fracture pattern and the location of the fracture origin.

2.6.1 Internal pressure resistance (IPR)

The crack pattern of a glass bottle broken due to hydraulic pressure provides information on the fracture pressure. After glass bottles are pressurized to failure, the highest reached internal pressure can be estimated by analysing the glass fragments. While increasing the pressure inside the glass bottle, the stored energy will increase proportionally. A higher stored energy will result in a higher crack density because the energy is converted into the additional surface area.

Whenever a high amount of crack branching is observed, high test pressure has preceded the fracture (Figure 10). The length of the cracks can be predicted, knowing that the length varies inversely with the square of the applied stress [25]. The initiation of the crack usually starts on the outside wall of the bottle as the chances of the appearance of imperfections are higher than on the inside wall. During the propagation of the crack, it will extend to the inside wall since the stress is slightly higher on the inside [27].

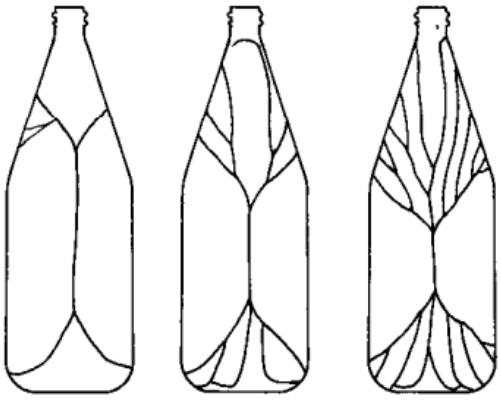

Figure 10: Pattern of fracture due to internal pressure at progressively greater pressures [27]

2.6.2 Topload pressure

The compression strength of glass can be more than ten times greater than its tensile strength, making fractures due to compression rare. As a result of inclined pores in the glass, which form open weak spots through which stress lines cannot pass, lateral tensile stresses occur locally. Due to the tensile stresses, microcracks, also called wing cracks, are formed and subsequently grow stably. The microcracks change the stress lines so that the local tensile stresses will orient horizontally. The microcracks will spread and align themselves parallel to the axis of compressive stress. As long as the compression continues, microcracks will continue to form until the specimen becomes saturated. A sudden collapse of the structure will lead to permanent fracture. Thus, the strength of glass against load is not determined by a single weak spot, but rather by its density and distribution [27].

2.6.3 Impact resistance

The fracture behaviour can less easily be predicted when fracture as a result of impact occurs. In addition, the variation in the velocity of the impact required for a bottle to break will be greater than the variation in the required pressure to fracture a bottle. The variation in impact velocity is a result of a significant thickness variation both between and within bottles [25]. Fractures due to an external impact on the side wall of the bottle often show a starburst pattern at the site of impact (Figure 11). Whether the crack branching starts at the inside or outside of the impact site depends on the sharpness of the impactor. However, the fracture origin is not necessarily located at the impact site. The force of the hammer's impact can cause the side wall of the bottle to bend outward, creating bending stress at the side wall, which leads to hinge fractures. From the hinge origins, a leading crack can propagate to the point of impact. This can initiate or exacerbate fragmentation at the impact site [27].

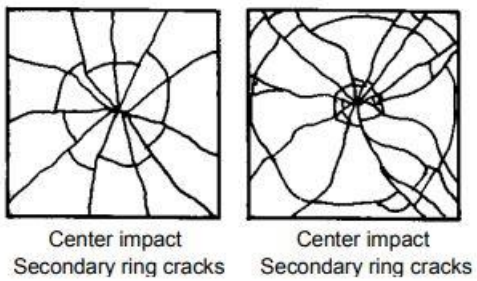

Figure 11: Fracture of centre impact [27]

Impacts with a blunt object form Hertzian cone cracks in the glass, which begin as a ring just outside the contact area between the two bodies. The load and the geometry of the blunt object and the elastic properties of both bodies determine the size of the contact surface. The surface of the glass specimen should be examined after contact damage. Witness traces can occur both at the contact site and at other impacts nearby, although the marks will be as visible as marks of impacts with sharp objects.

Increasing the impact velocity results in a significant decrease in included cone angle (Figure 12), which makes it possible to estimate the impact velocity based on the cone angle. The area of the footprint that is left behind depends on the load of the impact. A high load will expand the footprint area and will leave multiple concentric rings and cone cracks behind [27].

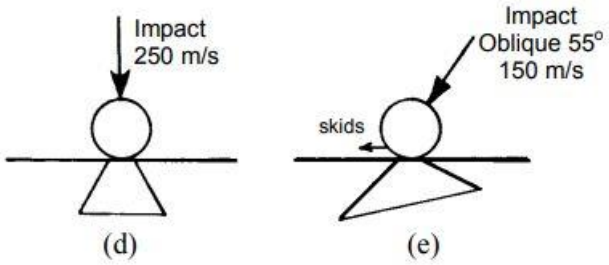

Figure 12: Blunt impact cone crack profiles [27]

3. Materials & methods

All tests were conducted in a conditioned lab, with the temperature maintained at 23°C and the relative humidity at 50%. Glass bottles were conditioned for at least 24 hours before tests are performed on them.

3.1 Types of returnable glass bottles

The tests were performed on different types of returnable glass bottles. Both bottle A and B have a capacity of 33 cl. They differentiate themselves in shape and colour. Figure 13 shows the technical drawing of both returnable bottles with the height and diameter indicated.

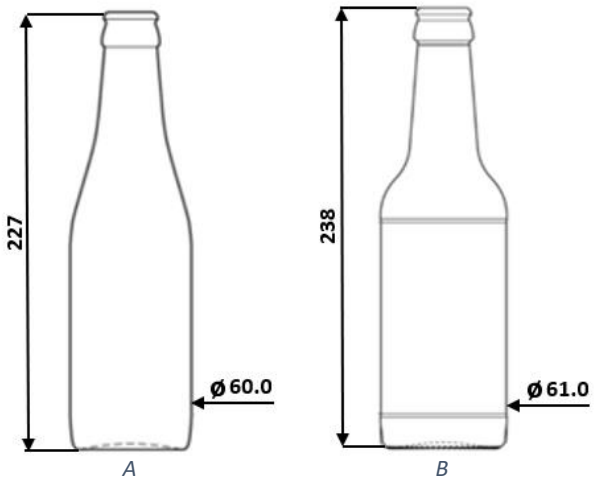

Figure 13: Technical drawing of returnable bottles A and B [2]

On the heel of each bottle, there is a code [28] displayed with more information about the manufacturer of the bottles, through a manufacturer's symbol together and a plant ID. The cavity identification number, in combination with a matching dot code (Figure 14), and markings as required by legislation including measuring container requirements are part of the required information. Besides, the bottle code may include the year of manufacture and identification of the mould [23].

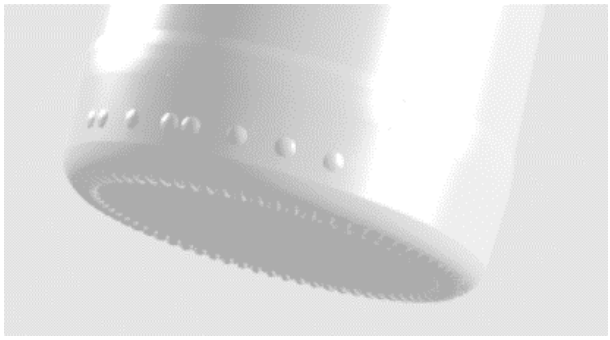

Figure 14: Dot code of cavity identification number [29]

During the study, the cavity identification number of each bottle was tracked. If the bottles of a particular cavity number show large deviations from the other bottles, this information can be passed on to the producer of the bottles. The producer can then further investigate where the problem lies and the bottles can be taken out of production if needed.

3.2 Neat bottles as reference

The Ramp Pressure Tester 2 (Agr International, Inc., USA) (RPT 2), shown in Figure 15, was used according to the standard ASTM C-147 to apply internal pressure to glass containers, such as glass beer bottles. The RPT 2 was operated in different testing modes. A properly executed verification using a test gauge ensured that the accuracy of the device was maintained.

Figure 15: Ramp Pressure Tester 2 [30]

3.2.1 Destruction IPR test

The first testing mode using the RPT 2 was the *Destruction IPR test*, which was performed to measure the maximum internal pressure resistance (IPR) that a bottle can resist. During this test, an empty bottle is clamped into the RPT 2 before closing the door to the testing station.

The device automatically starts to fill the bottle with water and seals it afterwards. The hydrostatic pressure inside the bottle increases at a uniform rate until failure, with a maximum test limit of 60.0 bar. When the maximum IPR value of the bottle is exceeded, it breaks and the shards are collected in a cullet collector (Figure 16). The collection of the shards allows possible further investigation. After bottle breakage, the one-minute equivalent pressure of the maximum internal pressure reached is displayed. Bottles that withstood pressures higher than 60.0 bar do not break and are removed from the unit as a whole [30] [31].

Figure 16: Bottle before (a) and after (b) breakage as a result of Destructive IPR test

The *Destruction IPR test* was executed on a series of 50 neat bottles each of types A and B. The average and the standard deviation of the results per type of bottle were taken as a reference for the strength of the bottles.

3.2.2 Analysis of the fracture origin

After the breakage of the bottle as a result of the *Destruction IPR test*, the shards collected in the cullet collector were analysed through fractography. The analysis of shards after a fracture (see paragraph 2.5.3) provided a lot of information about the fracture. Since the excessive internal pressure was the cause of the fracture, the fracture pattern looked like the patterns shown in Figure 10. The amount of branching that occurred corresponded to the amount of failure stress. The higher the pressure increased during the *Destruction IPR test*, the more branching occurred during the fracture. High branching increased the number of shards, making the analysis of the shards more difficult. A large number of smaller pieces of glass complicated the search for the pattern and the origin of the fracture.

Marking the heel contact and the shoulder contact of the bottle in different colours (Figure 17) helps to better understand the orientation of branching shards after breakage. The heel contact marks the line between the heel and the label panel, whereas the shoulder contact is located between the label panel and the shoulder. Markings made it easier to determine whether a fracture origin was located in the heel or below, between the heel and the shoulder, or in the shoulder or above by tracing back the branching to the origin.

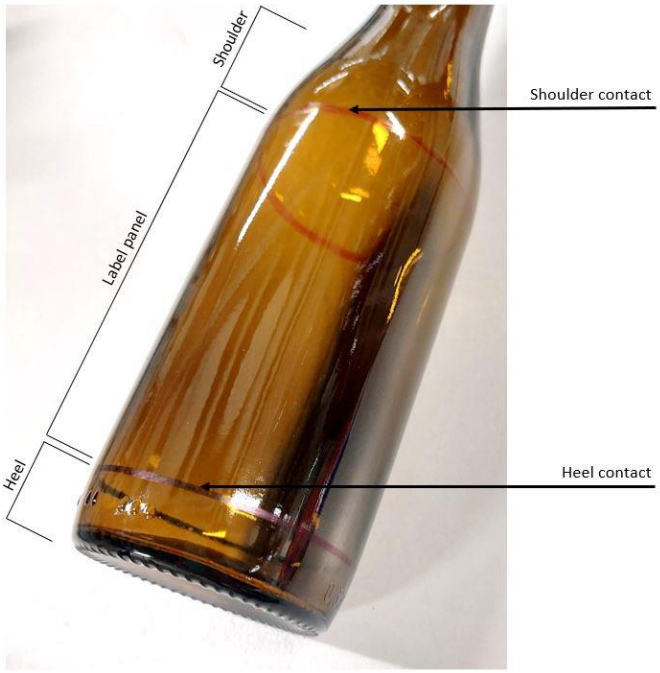

Figure 17: Markings on heel contact and shoulder contact

The branching pattern leads back to the origin of the fracture. By puzzling the shards back to the place in the bottle where they came from, the shards containing the origin are found. These shards usually consist of a typical shape that depends on the reason for the breakage. For fractures due to internal pressure, shards in the shape of butterfly wings or a saddle are expected. To guarantee the origin is located in these shards, phenomena such as mirrors, hackle lines, and haze, which are typically located at the site of the cause of the fracture were looked for in the thickness of the glass. The examination of fracture surfaces was done using the unaided eye or using a simple magnifying glass. Surfaces that were dried with a paper towel were easier to examine. Every operator has to gain experience in the study of the fractured surface and recognition of different fracture patterns gradually over the years [27].

3.3 Static simulated stress

3.3.1 Internal pressure resistance (IPR) through frozen water

The first method for applying internal pressure was based on the expansion of water at temperatures below 0 °C. Bottles were filled with water to different heights starting at 3 cm measured from the bottom and increasing with 1 cm up to 15 cm. Five filled bottles per height were frozen in a freezer or climate cabinet (Weiss Technik, The Netherlands) at a temperature of −18 °C. The water in the bottle thereby expands and applies internal pressure to the bottle (Figure 18) for several hours. However, the pressure is only applied to the part of the bottle below the water level. No pressure is exerted on the top part of the bottle where there is no water touching the wands. Whenever the internal pressure exceeds the maximum internal pressure the bottle can withstand, the bottle breaks inside the freezer or climate cabinet. For that reason, the bottles were placed inside plastic zip-lock bags to collect the shards. After the analysis of the number of broken bottles per filling height, it becomes clear which places in the bottle, depending on height, are more sensitive to internal pressure.

Figure 18: Internal pressure due to the expansion of frozen water

Based on these results, the two highest levels without fracture were chosen to carry out further tests. Two series of 50 bottles were filled to the two highest levels and frozen in the climate cabinet at −18 °C for at least 18 hours. Ideally, no more breakages occurred so that all bottles could be taken out of the climate cabinet intact. The water in the bottles was thawed and the bottles were emptied. Subsequently, a *Destruction IPR test* was carried out on these 50 bottles using the RPT 2. The results were compared with the reference values to see if the strength of the bottles has decreased due to the expansion of the water. The shards were analysed (see paragraph 3.2.2) to determine whether there has been a shift in the location of origin.

3.3.2 Internal pressure resistance (IPR) through a Proof IPR test

A second method for applying internal pressure was only performed on type A bottles. To start, the test mode of the RPT 2 was set to a *Proof IPR test*. During a *Proof IPR test*, a required pressure was set. After the bottle was filled with water and sealed, the hydrostatic pressure increased until the set value was reached. The result of this test was either pass or fail, depending on whether or not the bottle broke under the set pressure. Bottles that passed the *Proof IPR test* at a certain set pressure were removed in one piece [30] [31]. Compared to tests that apply internal pressure to the bottles through frozen water, internal pressure is applied for only a few seconds during the *Proof IPR test*. These pressures have a higher value so that the applied load would correspond to a lower pressure for a longer period of time.

A pressure of 15.0 bar, 20.0 bar, and 25.0 bar was applied to a series of 30 bottles each. The bottles that survived this *Proof IPR test* were taken out of the device as a whole and subsequently measured through a *Destruction IPR test* to see if the obtained pressures from the *Proof IPR test* had affected the strength of the bottles.

3.3.3 Topload pressure

To simulate a topload pressure in lab conditions, the Vertical Load Tester (VLT) as shown in Figure 19, which is compatible with the RPT 2, was used. The test analysed the maximum pressure or weight a bottle could support without breaking, by applying vertical pressure on top of the bottle (Figure 20).

Figure 19: Vertical Load Tester [32]

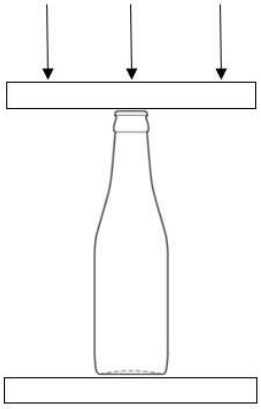

Figure 20: Principle of topload pressure

To simulate a stacking load, the glass bottle was fitted with a crown cap and placed in the proper size cullet can (Figure 21). This cullet can was placed inside the VLT, which would apply the topload pressure to the can and therefore to the bottle. The RPT 2 was used to set the desired test pressure that the VLT would apply. The pressure on top of the bottle increased at a uniform rate, with a maximum destruction load of 20,007 N. Through this test, a large load is applied for a few seconds, corresponding to a smaller load that occurs in the life cycle of the bottles for a longer amount of time. The device detected failure from an increase in height of 0.15 cm. If the bottle broke under the topload pressure, the shards were collected in the can. Bottles that withstood the applied pressure remained intact and were removed as a whole [32] [33].

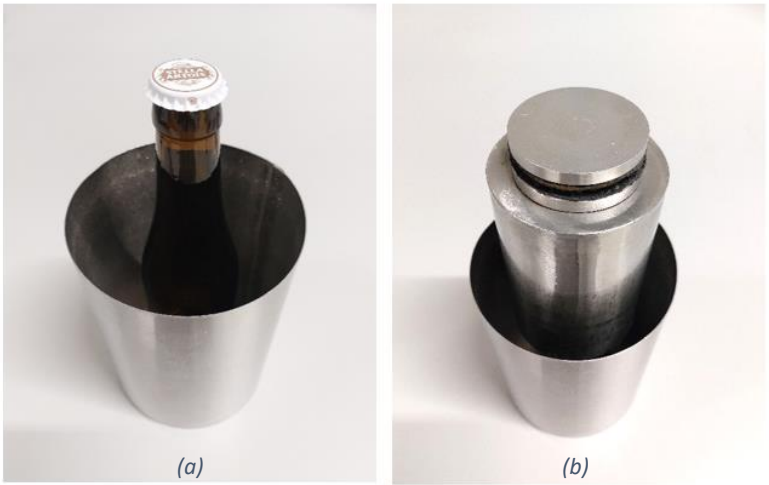

Figure 21: Bottle with crown cap inside cullet can without (a) and with (b) upper lid

To analyse the effect of topload pressure on the strength of bottles of type A, a series of 30 bottles was subjected to a *Destruction VLT test* at 20,007 N. To perform even higher pressures on the bottles, an additional set of 30 bottles was subjected to the same test eight times. The bottles that were still intact after the test, underwent a *Destruction IPR test*. The average IPR values on one time and eight times a 20,007 N load were then compared with each other and with the reference value, to conclude the effect of topload pressure on the strength of a bottle.

3.3.4 Impact resistance

Impact was applied to type A bottles using different equipment and different methods to choose the most correct test method for the application of impact from the comparison. Thus, both a manual (Figure 22) and an automatic impact tester were used. In both methods, the glass bottle was held firmly while a pendulum impacted the bottle (Figure 23). Depending on the height at which the pendulum was released, the force of the strikes would vary. The initial impact always starts at a force of 50 CPS (cm/s). After the first strike, the bottle rotates around its axis at a certain angle, so that a different place was struck each time. The bottle keeps rotating after each strike until it has rotated completely and the pendulum is back at the level of the first impact. Then, the force is increased by 10 CPS, and the same steps are applied. The force keeps increasing until a fracture occurs. The force at which the last impact is administered, with a limit of 320 CPS, is noted so that the different test methods can be compared.

Figure 22: Manual Impact Tester [34]

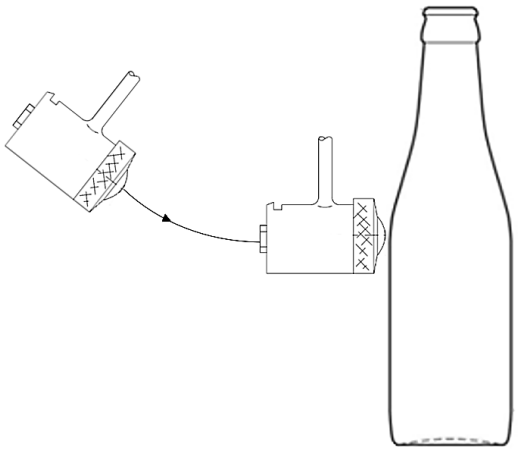

Figure 23: Pendulum impacting bottle at shoulder height

Several series of 30 bottles each were tested with a different angle between the strikes each time, namely 30° with the manual impact tester and 30°, 45°, and 120° with the automatic impact tester. All impact tests were carried out in such a way that the pendulum stroke at shoulder level which measures at 103 mm from the bottom of the bottle.

After finding the optimal test method, the following tests on the effect of an impact on a glass bottle were carried out. The pendulum strikes the shoulder at the exact same place several times with the same force. To check the effect of the number of strikes, the force remained at 100 CPS, while the number of strikes varied between 50, 100, and 150. For the effect of the force, the same principle was

used. The pendulum stroke 100 times each time, while the force varied between 50 CPS, 100 CPS, and 150 CPS. Each series of tests was carried out on 30 bottles. After impact application, all bottles that survived the force were tested using a *Destruction IPR test*. The results were compared with the reference values of the neat bottles to find out the effect of impact. In addition, the results from each series of bottles were also compared with each other to see if the number of impacts and the force with which the pendulum stroke affected the strength of the bottle.

Before having the bottle broken by the *Destruction IPR test*, the place where the pendulum stroke and the two places where the anvils had held the bottle stable were marked (Figure 24) since the fracture was expected to occur at one of these specific locations. After the fracture, the markings made it easy to verify that the fracture origin was located at the point of impact.

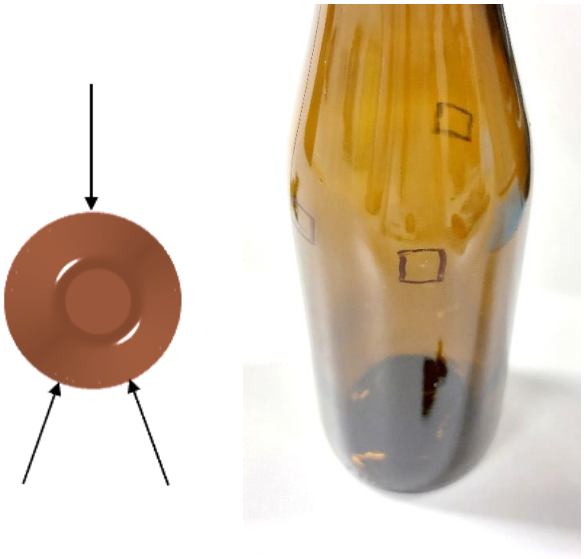

Figure 24: Markings after application of impact

3.4 Dynamic simulated stress

3.4.1 Line simulation

To simulate the effect of a conveyer belt where bottles will contact each other, a line simulator (Figure 25) was used. This method simulates the abrasive effects of the production lines. The number of bottles that were placed inside the circular device depends on the diameter of the bottles. For type A, 28 bottles were used to fill the line simulator, while still leaving enough place between them so that the contact between bottles could be broken and then restored. For type B, 24 bottles are placed inside the line simulator for each test. The bottles were guided between two concentric circles of non-abrasive material, to make sure that all damage is a result of bottle-to-bottle contact. A gate with an adjustable opening ensured that the circular path followed by the bottles deviated. This deviation of the path created a certain slip rate that reflected the speed of the bottles relative to the moving belt. The bottles moving through the gate created a rotational movement against other bottles, causing friction to the contact surface [35]. After the bottles are removed from the line simulation, they have to rest for at least 24 hours so that all damages can normalize.

Figure 25: Line simulator [35]

This test could be performed on both empty and filled bottles, depending on the state of the transportation on the conveyer belt that is recreated, which can be either before or after the filling. It is also possible to have water sprayed over the bottles during the line simulation.

A line simulation with a rotational speed of 60 RPM performed for 5 minutes corresponds to the damage incurred during the effective life cycle of the bottles in terms of friction and impact [35]. To analyse the effect of the rotation speed of the moving belt during a 5-minute line simulation, the same test was carried out on type A bottles at different rotation speeds: 30 RPM, 45 RPM, and 60 RPM. Besides the effect of rotation speed, the effect of the duration time was investigated. The rotation speed of the moving belt was kept constant at 60 RPM, while the time was varied between tests. The line simulation was performed with a test time of 2.5 minutes, 3.75 minutes, and 5 minutes. All tests were carried out on a series of 28 filled type A bottles, to fill the line simulator while leaving a small gap for contact to be broken and restored. To check whether the effect of duration time is the same for different types of bottles or whether there is a difference in the results due to the different shapes of the bottle, the tests at a constant speed of 60 RPM were also performed on 24 type B bottles. This time with a duration time of 30 seconds, 1 minute, 2 minutes, and 5 minutes. The slip percentage of the gate was kept constant at 40% during all tests and there was a constant supply of water coming from the spray head.

After the line simulation, all bottles were tested using a *Destruction IPR test*, to analyse the reduction of the strength of the bottles. A final test was performed at a speed of 60 RPM for 5 minutes. After this test, unlike all previous tests, there was no waiting for 24 hours after the line simulation, but the bottles were dried to immediately perform a *Destruction IPR test*.

3.4.2 Scuffing simulation

Because during the line simulation not only friction occurs due to the contact between bottles, but also impact because the contact between the bottles is broken and restored, scuffing simulations were performed on type A bottles. The scuffing simulation aimed to keep the impact as limited as possible and, in this way be able to analyse the effect of the friction individually.

During a scuffing simulation, two bottles are pushed against each other with a certain pressure while the bottle is rotating around its axis. One of the bottles rotates clockwise, while the other one rotates counterclockwise. Each rotation speed is set individually. The pressure squeezing the bottles together is set and maintained during the whole simulation. To minimize the impact between the two bottles, the pressure is set to the lowest value which could still ensure constant contact between the bottles.

This means that when the shape of the bottle deviates slightly from the expected round shape, the position of one of the bottles adjusts to hold the bottles together at the same pressure. The bottles perform a one-time impact on each other during the first contact. After that, the contact does not break and no more impacts occur.

During the simulation, the left bottle was tilted at an angle of 45° (Figure 26). During tilted scuffing, not the entire label panel surface was scuffed, but only the circumference at one particular height located in the label panel. The left bottles were kept separate from the right bottles to retrospectively observe the effect of the tilt on the left bottle.

Figure 26: Angle of 45° between the bottles during scuffing simulation

A scuffing simulation was applied to a series of 30 bottles for 10 minutes. The bottles were pushed together at a pressure of 2 bar and had a rotation speed difference of 40 RPM. One bottle rotated clockwise at 20 RPM, while the other one rotated counterclockwise at 60 RPM. One of the two bottles was tilted at a 45° angle so that scuffing only occurred at a height of 65 mm, located in the label panel. After the scuffing simulation, all 30 bottles were tested using a *Destruction IPR test*. Before doing so, the circumference of the bottle that was scuffed was marked (Figure 27), making it easier to find out if the bottle broke due to the scuffing or broke somewhere else in the bottle.

Figure 27: Marking after scuffing simulation

3.5 Design of Experiments

During the first approach to combine the different loads that are applied to the bottles in their life cycle, friction, topload pressure, and impact were chosen as the three main factors and applied to type A bottles. Internal pressure is not included in the combination as it is chosen to be the reference for the strength of the bottles and to minimise the number of factors and keep the processing of the results. Five different runs were tested to analyse the effect of each factor and each possible combination of factors. After the application of the factors in question, the bottles are tested through a *Destruction IPR test*. Table 1 shows the five runs, for which 28 or 30 bottles were tested each time, depending on the devices used to apply the factors in question.

- Run 1 only measured the effect of pressure, more specifically topload pressure. These results are therefore replicated from the previous test regarding the measurement of the effect of a topload of 20,007 N.
- Run 2 measured only the effect of impact. Again, these results were carried over from a previous test. The effect relied on the results of the test where an impact with a force of 100 CPS struck the bottle 100 times at the same location.
- Run 3 measured the effect of the combination of impact and friction through a line simulation. Here, the results were carried over from the test where the line rotated at a speed of 60 RPM for 5 minutes with a slip rate of 40% and the *Destruction IPR test* was carried out 24 hours later.
- Run 4 measured the effect of the combination of topload pressure and impact. This involved first applying an impact of 100 CPS to the 30 bottles measured 100 times, the same amount as in Run 2, and then applying a topload pressure of 20,007 N, the same amount as during Run 1, to the same bottles.
- Run 5 measured the effect of the combination of the three factors. The 28 measured bottles first underwent a 5-minute line simulation at a speed of 60 RPM and a slip rate of 40%, as in Run 3. Then a topload of 20,007 N was applied, as in Run 1, to the same 28 bottles.

Table 1: Approach to testing the combination of friction, topload, and impact

	Run 1	*Run 2*	*Run 3*	*Run 4*	*Run 5*
n	*30*	*30*	*28*	*30*	*28*
Friction			*x*		*x*
Topload	*x*			*x*	*x*
Impact		*x*	*x*	*x*	*x*

Based on the results of Run 2 and Run 3, an estimate was made about the effect of friction individually. However, this was an estimate since it was not possible to say with certainty from the line simulation results how large the proportion of impact and friction individually are on the total effect. To assume that the effect of friction would effectively be the estimated value, there would have to be exactly as much impact on the bottles during the line simulation as was applied during Run 2.

By analysing the results of Run 2 and Run 5, the effect of the combination of pressure and friction was also estimated.

Since this first approach was only an estimate of the effects that friction, pressure, impact, and the combination of the foregoing, a full Design of Experiments (DoE) was performed. During the testing of each factor, a high and a low value were chosen, as shown in Table 2. The other device settings were kept constant during the testing. The lower values were chosen to be as close to the standard [23] as

possible. The standard notes that a returnable glass bottle should be able to withstand a topload of 6002 N and an impact of 89 CPS. The higher values were chosen to be 1.5 times the lower value.

Table 2: High and low values used during the DoE

	-1	*+1*	
Friction	*10 min*	*15 min*	*At a constant rotation speed differential of 40 RPM, a constant pressure of 2 bar and where one of the two bottles was tilted at a 45° angle*
Topload	*6002 N*	*9003 N*	
Impact	*100 strokes*	*150 strokes*	*At a constant force of 89 CPS at shoulder level*

To perform a full DoE of three factors, eight runs were needed to make sure all the different combinations of low and high values are tested. Table 3 shows the different setups of the eight runs. The order in which friction, topload, and impact are applied is the same for each run and is based on the actual loads that occur on the bottles during their life cycle, to deliver the most accurate results. Friction is always the first load applied, as friction occurs between the bottles during transport to the filler on the conveyor belt. After the filler, the bottles will end up on the conveyor belt several more times, but to analyse the effect and interactions of the factors, friction is applied only once during the DoE. Friction is succeeded by topload pressure, which occurs during the filling and capping of the bottles. Lastly, impacts are applied to the bottles corresponding to the impacts the bottles receive during the labelling and packing.

Table 3: Approach of the DoE

	Run 1	*Run 2*	*Run 3*	*Run 4*	*Run 5*	*Run 6*	*Run 7*	*Run 8*
n	*30*	*30*	*30*	*30*	*30*	*30*	*30*	*30*
Friction	*-1*	*-1*	*-1*	*-1*	*+1*	*+1*	*+1*	*+1*
Topload	*-1*	*-1*	*+1*	*+1*	*-1*	*-1*	*+1*	*+1*
Impact	*-1*	*+1*	*-1*	*+1*	*-1*	*+1*	*-1*	*+1*

After friction, top load pressure and impact have been applied to the bottles, all bottles were tested with a *Destruction IPR test*, from which the average IPR value was obtained in each case. The individual effects of the three factors then were extracted from the results obtained. This made it possible to compare so that the factor with the most influence on the strength of the bottle could be concluded. In addition to the different effects, the interactions between these effects were examined to determine whether they influence each other.

4. Results and discussion

4.1 Characterization of the reference neat bottles type A and B

In this study, the returnable bottles are tested for their internal pressure resistance (IPR) since they are subjected to internal pressures several times during their life cycle. Bottles that are filled with a carbonated drink have felt internal pressure while filling. The pasteuriser also creates internal pressure on the bottles. In fact, the pressure the bottles undergo during the pasteurisation is for most bottles the greatest pressure they will experience in their lifetime. Lastly, storage can create internal pressure in special circumstances. This only applies to overfilled bottles, in which too little headspace is provided.

The IPR values were obtained using a *Destruction IPR test* with the Ramp Pressure Tester 2 (RPT 2) on neat bottles of each type. The average of the IPR values will be taken as a reference to which values measured further on will be compared. From the comparison with the reference values conclusions can be drawn about the extent to which the strength of a bottle is influenced by a certain treatment.

To provide enough bottles throughout the entire study, multiple pallets of both types of bottles were delivered. To guarantee that there are no significant differences between the two shipments of bottles, a series of bottles from each pallet was tested. The results of type A bottles are shown in Table 4 and the results of type B bottles are shown in Table 5.

Table 4: IPR (bar) of neat bottles A

	Bottle A - Run 1	*Bottle A - Run 2*	*Bottle A - Total*
n	*50*	*50*	*100*
Average (bar)	**37.7**	**38.4**	**38.0**
Stdev	9.2	10.9	10.0
Min	18.9	17.3	17.3
Max	58.8	59.6	59.6

Since there are no significant differences between the two series of results of bottle A, they will be combined. All further tests will be compared with the average of the total series of values.

Table 5: IPR (bar) of neat bottles B

	Bottle B - Run 1	*Bottle B - Run 2*	*Bottle B - Total*
n	*50*	*48*	*98*
Average (bar)	**42.2**	**27.2**	**34.8**
Stdev	11.1	7.6	12.1
Min	19.4	13.9	13.9
Max	> 60.0	47.0	> 60.0
# not broken	3	/	3

The two runs of neat bottles of type B differ significantly with a p-value below $2 \cdot 10^{-11}$ as a result of a t-test with 95% reliability. Since the standard deviation would be too high when the two runs are combined, they will be kept separate. Results obtained further in the study will always be compared with the run from the same shipment. Thus, the comparison with the reference values will be more accurate and the effect of a given treatment will be more measurable.

Since there is a limit of 60.0 bar for the tests performed with RPT 2, there are some bottles that will not break during the test. These bottles can handle an internal pressure higher than the output pressure of 60.0 bar. Because the effective pressure required for rupture is unknown, these values cannot be included in the calculation of the mean and standard deviation but will be included as a value of 60.0 bar. As a result, the effective values for both the average and the standard deviation for bottle B – Run 1 will be slightly higher than shown in Table 5, as 3 of the 50 bottles have not broken at a pressure under 60.0 bar.

The average IPR values of the two types of bottles are fairly high, knowing that the target for returnable bottles lies at an average of above 25 bar [23]. This means that the production of these returnable bottles was successful in terms of resistance against internal pressure. The minimum IPR value that a returnable bottle should be able to resist depends on the carbonation level of the beer that will be stored in these bottles. For carbonation levels between 3 g/L and 6 g/L, the minimum pressure per individual bottle lies at 12 bar [23]. Bottles that break at a pressure lower than 12 bar are labelled out-of-specification (OOS). In this series of neat bottles A and B, all bottles fall within specifications.

The strength of the glass bottles is set by the flaw severity and the loads that have been applied to the bottles. Neat bottles have not yet experienced any loads, except during storage and transport, which means the inherent flaws set the strength that was measured through IPR.

The standard deviations on the results of more than 10 bar are quite high compared to the averages but are similar for the different types of bottles. For glass bottles, a high standard deviation is to be expected since the strength is a result of the flaw severity, which will be different for each produced bottle. It is generally assumed that all results of glass bottles are normally distributed, with both ends of the bell curve truncated. The truncation is a consequence of the pre-sorting by the supplier and the test limit. To validate this assumption, a normal distribution of IPR values can be plotted. Since the values for bottle B exceed 60.0 bar and the normal distribution would therefore fall outside the range with a limit at 60.0 bar, it is not possible to compare the values with their normal distribution. For neat bottle A, the actual distribution of values is compared with the probability of the normal distribution based on the average and standard deviation, as shown in Figure 28.

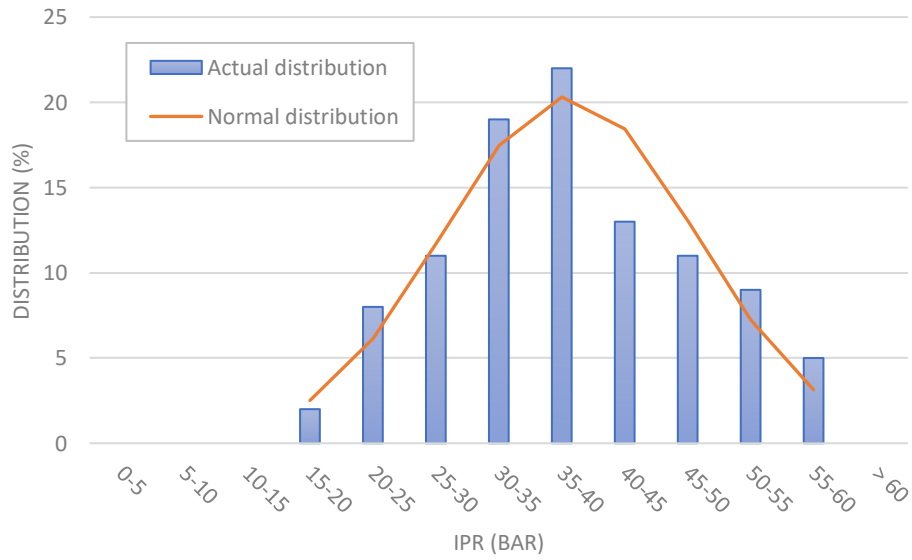

Figure 28: Normal distribution of IPR (bar) of neat bottles A

The results of neat bottle A are consistent with the expected bell curve. Due to the large number of tested bottles, both graphs coincide nicely.

For the set of results of neat bottles A – Run 1 and neat bottles B – Run 1, each broken bottle was checked for the origin of the fracture. The fracture origin is located where the worst combination of stress and flaw severity occurs. This means that a flaw could have been present at the fracture origin. To find out whether the bottles have a weak spot where most of the fractures occur or the distribution of the locations of the fractures are scattered, the orientations of the origins are shown in Figure 29.

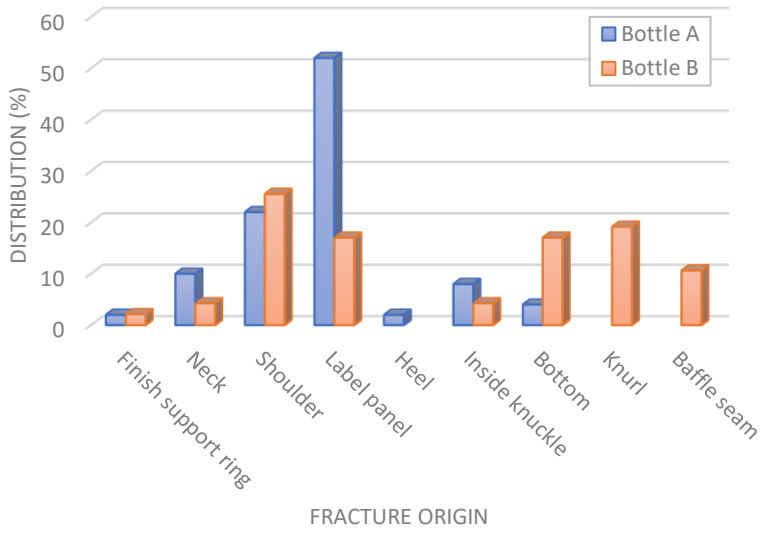

Figure 29: Distribution of fracture origins of neat bottles A and B

The results show that most fractures of bottles A have an origin located in the label panel (Figure 30) of the bottle. The shoulder (Figure 30) is also a common site for fracture origins. Other locations or only occasionally the point of origin.

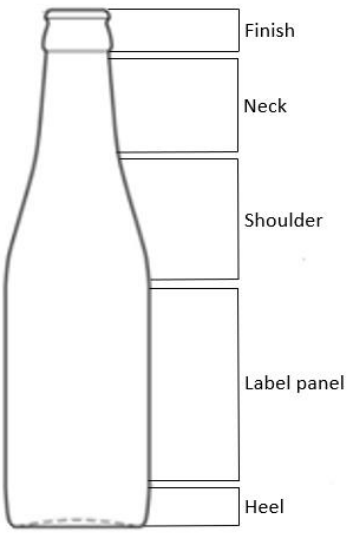

Figure 30: Areas at front view of bottle

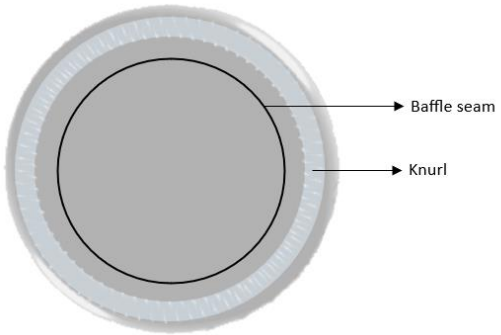

Figure 31: Areas at bottom view of bottle

It is a possibility that the bottles have suffered the most damage at the shoulder and the label panel during production and transportation. However, the fact that the region that is regarded as the label panel has the largest relative surface area should be taken into account. Therefore, a fracture origin has a good chance of being located in the label panel. In contrast with the label panel area, the finish support ring (Figure 30) only takes up a small area of the bottle, which decreases the chances of a fracture origin being located there. The analysis of the distribution of fracture origins relative to the areas shows that the origins seem to be well distributed throughout the entire bottles of type A. Bottle B contrasts with these results, as the fracture origins of bottle B are not regularly distributed throughout the entire bottle. The label panel, the bottom, and the knurl contain the same amount of fracture origins, despite the difference in relative area. There are proportionally more bottles with a fracture origin located in the bottom, baffle seam, and knurl (Figure 31), also called the bearing surface. This could indicate an imperfection in the mould or a problem in the cooling process of the bottles.

4.2 Effects of static simulated stress

During further testing, stress will be applied to the bottles through internal pressure, topload pressure, and impact to simulate potential events during a bottle's life cycle, such as the pasteurization, capping, and labelling. The application of these factors may induce additional defects to the glass which can reduce the strength of the bottle. All test methods will end with a *Destruction IPR test* to make sure the obtained average IPR can be compared with the reference IPR value of the neat bottles. Based on this comparison, the effect of applying internal pressure, topload pressure, and impact can be determined.

4.2.1 Internal pressure resistance (IPR) against frozen water

For the tests based on the expansion of water at freezing temperatures, the highest level at which the bottles could withstand the internal pressure needs to be determined. Five bottles per level were filled and frozen in the freezer or climate cabinet.

The different levels tested depend on the size and shape of the bottle, based on the hypothesis that the bottle can withstand the smallest internal pressure around the flexion of the shoulder. Bottle A has a capacity of 33 cl and will, therefore, be filled up to different levels starting from 7 cm and going up to 13 cm, with a 1 cm difference each time. Bottle B has the same capacity and was therefore filled up to the same initial level of 7 cm. Bottles were filled for every 1 cm more going up to 15 cm since the shape of the bottle is different. The curvature of the shoulder starts at a higher point than at A. Bottles filled up to 14 cm and 15 cm will therefore also be tested.

To begin with, the different bottles of type A were frozen in the freezer at −18 °C. When they were taken out of the freezer after 20 hours, the bottles still contained liquid water and only partially solid ice. The data from the logger also showed that the temperature of the water inside the bottle had only just reached −18 °C (Figure 32) and therefore had not had enough time to freeze. It can be concluded that the results from the bottles in the freezer are not reliable because the temperature and humidity vary greatly in different places in the freezer and it takes too long to make sure all the different levels of water are completely frozen.

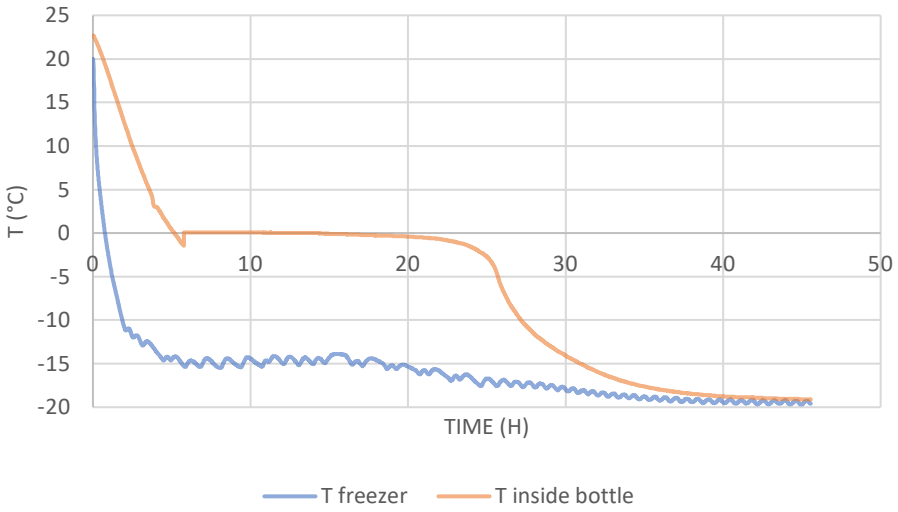

Figure 32: Temperature profile freezer (−18 °C)

The freezing of filled bottles for further tests took place in the climate cabinet of Weiss Technik since there is better airflow and no moisture is present. The measured temperature profile in the climate cabinet (Figure 33) is therefore much smoother than in the freezer. The temperature reaches the end point of −18 °C faster, after approximately 18 hours, and remains stable at this temperature.

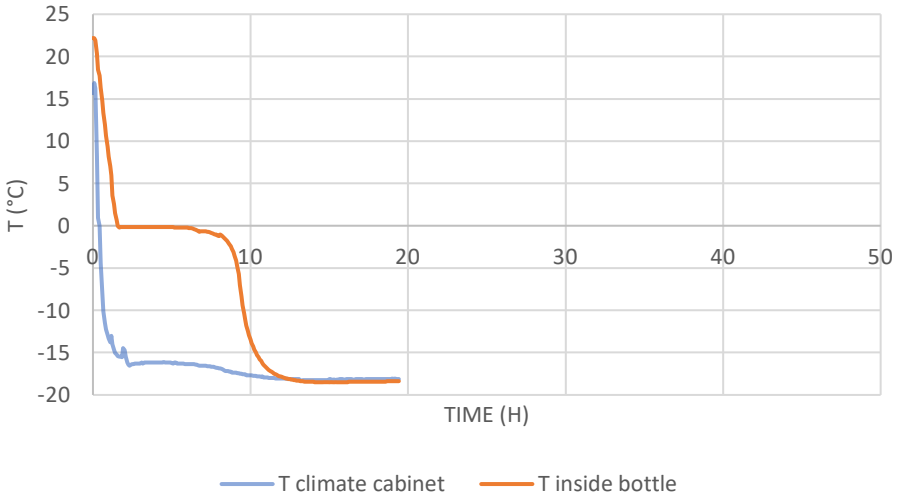

Figure 33: Temperature profile climate cabinet (−18 °C)

The tests of bottle A at different levels from 7 cm to 13 cm were not repeated in the climate cabinet. An estimate was made for the two highest levels without breakage based on the results of the other type of bottles. All levels of bottle B have been frozen in the climate cabinet. Table 6 shows the height and volume of the most accurate results for each type of bottle.

Table 6: Failure height (cm)

	Bottle A			*Bottle B*		
	Freezer			*Climate cabinet*		
Height (cm)	*V (ml)*	*n*	*# broken*	*V (ml)*	*n*	*# broken*
7	146	5	/	142	5	/
8	172	5	/	168	5	/
9	194	5	/	192	5	/
10	222	5	/	214	5	/
11	248	5	/	240	5	/
12	270	5	/	260	5	1
13	290	5	1	280	5	5
14				300	5	4
15				310	5	5

The two highest levels of water without fracture are 10 cm and 11 cm for bottle B. For bottle A an estimate is made based on the results of level B since these bottles have the same capacity, which means 10 cm and 11 cm will be chosen as the two highest levels.

Based on the results of Table 6, the two highest levels without fractures were obtained or estimated. For a *Destruction IPR test*, a total of 50 bottles per height for each type of bottle is needed. Due to the limited number of available bottles, some levels have less than 50 samples for the *Destruction IPR test*. The estimate for the level of bottle A turned out to be wrong. The bottles filled to 10 cm and 11 cm did break in the climate cabinet, in contrast to the freezer. Therefore, samples of levels 8 cm and 9 cm were made, which are used for further testing. The results after a minimum of 18 hours in the climate cabinet are shown in Table 7.

Table 7: Sample preparation for Destruction IPR test

	Bottle A			*Bottle B*		
Height (cm)	*n*	*# broken*	*%*	*n*	*# broken*	*%*
8	**29**	**1**	**3%**	**45**	**/**	**0%**
9	**50**	**/**	**0%**	**44**	**/**	**0%**
10	50	3	6%	**50**	**1**	**2%**
11	50	8	16%	**50**	**/**	**0%**

Most of the fractures that are caused during the freezing of the water are a result of the internal pressure in the bottle, which can be deduced from the fracture pattern. The origin of the fracture is usually located in the shoulder or the label panel of the bottle, but occasionally a fracture origin is oriented somewhere else in the bottle.

At the level of 10 cm and 11 cm, a few more ruptures occurred for bottle A. It can be concluded that the bottle will break when internal pressure inside the bottle occurs above 9 cm. This conclusion confirms the expectation as the shoulder of the type A bottle starts at 10.3 cm. The same conclusion can be drawn for type B bottles. An internal pressure in the bottle above 11 cm will cause the bottle to break, as the shoulder here starts at a height of 11.7 cm. The shoulder of the bottle can withstand less internal pressure due to the curvature of the bottle.

Although most of the ruptures were caused by excessive internal pressure, two out of three fractures of the bottles filled to 10 cm, were a result of impact. This can be inferred from the fracture pattern.

The impact creates a fracture in the form of a starburst (Figure 34), as opposed to fractures due to internal pressure, which begin in a vertical line that branches according to the amount of stress. There is a possibility that the bottles collided with each other or fell against another surface, causing them to sustain a fracture due to impact.

Figure 34: Fracture due to impact after freezing bottle A filled up to 10 cm

New samples were prepared for levels 8 cm and 9 cm, which were used for the *Destruction IPR tests*. After taking the frozen bottles out of the climate cabinet, all bottles were intact. After a certain amount of time, one of the bottles filled to a height of 8 cm still broke, as a result of sustained damage and chemical corrosion that reduced the strength of the damaged glass over time. Table 8 shows the results of the *Destruction IPR test* on bottle A for the samples filled up to 8 cm and 9 cm of water.

Table 8: IPR (bar) after freezing a certain level of water – Bottle A

	Bottle A		
	Neat	*9 cm water*	*8 cm water*
n	*100*	*50*	*28*
Average (IPR)	**38.0**	**36.2**	**35.0**
Stdev	10.0	8.3	9.4
Min	17.3	18.7	16.8
Max	59.6	52.2	53.0

The slight decrease in mean IPR values after applying internal pressure to the bottles to a height of 8 cm and 9 cm does not represent a significant difference in results concluding from the t-tests with 95% reliability with p-values of 0.14 and 0.26 respectively. Even though there is no significant difference between the average IPR values, the distribution of the frozen water results is compared with the normal distribution of the neat bottles (Figure 35 and Figure 36).

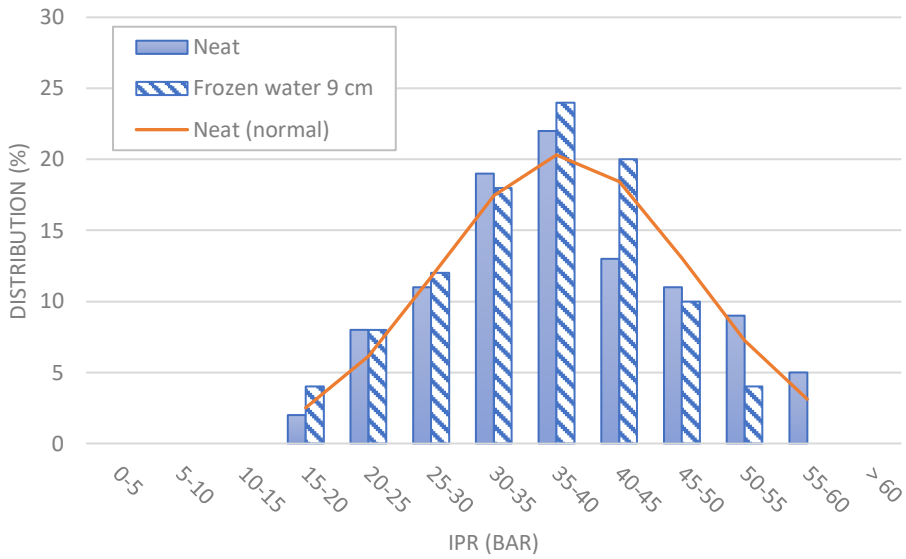

Figure 35: Distribution IPR (bar) after frozen water up to 9 cm – Bottle A

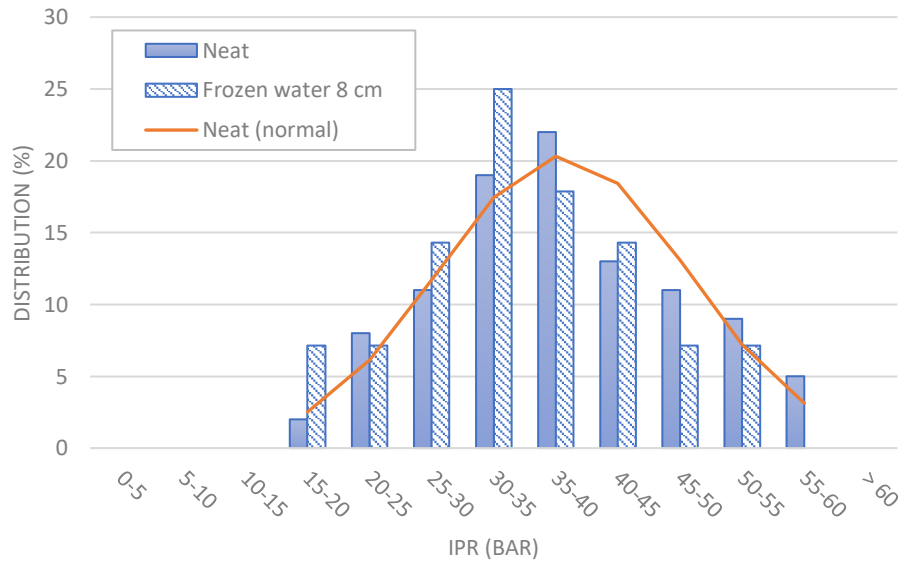

Figure 36: Distribution IPR (bar) after frozen water up to 8 cm – Bottle A

The distribution of the frozen water results of 9 cm shown in Figure 35 matches the distribution of the neat bottles. Figure 36 shows that there has been a slight, but no significant, shift in distribution of IPR values after 8 cm of frozen water. The distribution appears not to have changed shape despite the shift and still has the expected bell curve with both ends truncated.

Of the bottles that were filled to 9 cm and then tested with the *Destruction IPR test*, the origin of the fracture was checked for each break. Figure 37 shows the distribution of fracture origins of both the neat type A bottles and bottles A that were filled up to 9 cm.

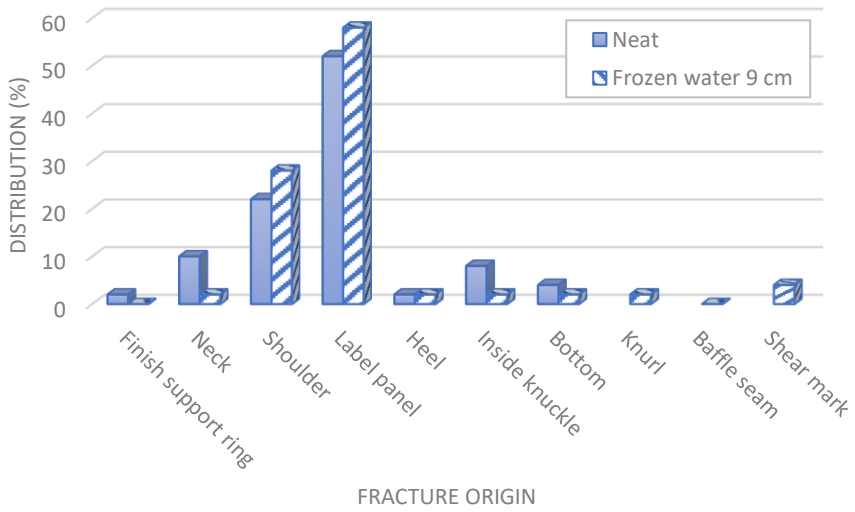

Figure 37: Distribution of fracture origin of bottle A, neat compared to frozen filled up to 9 cm

Figure 37 shows that the distribution of the fractures is the same for both cases and that the fractures always occur in the same places. This means that for the bottles that showed no difference in IPR values, there is also no difference in fracture origin distribution. It can therefore be concluded that type A bottles that are filled with water to a level of 9 cm or lower and of which the water subsequently freezes will not experience any negative effect from the internal pressure that occurred.

For bottle B, all four prepared levels are tested through a *Destruction IPR test*. Table 9 shows the results of the *Destruction IPR test* on bottle B for the four different levels of water, 8 cm, 9 cm, 10 cm, and 11 cm. The IPR values are compared with the neat bottles B of Run 1 since they are from the same production.

Table 9: IPR (bar) after freezing a specific level of water - Bottle B

	Bottle B				
	Neat	*11 cm water*	*10 cm water*	*9 cm water*	*8 cm water*
n	*50*	*50*	*49*	*44*	*45*
Average (IPR)	**42.2**	**41.0**	**38.8**	**39.5**	**38.3**
Stdev	11.1	10.7	8.6	9.9	10.5
Min	19.4	14.5	17.8	18.6	18.1
Max	> 60.0	> 60.0	56.5	> 60.0	58.7
# not broken	3	1	/	1	/

Over the span of the different levels, a slight decrease in average IPR value is noticed with a decrease in the height of water. However, it is 95% confident that there is no significant difference between any of the average IPR values when compared to the neat bottles or each other. This shows that the frozen water only affected the bottle at a height of over 11 cm. Below 11 cm, no differences can be observed with a change in water level.

During the *Destruction IPR test* of the series of 11 cm of water, the fracture origins of each bottle were analysed. The distribution of fracture origins after the 50 bottles were objected to 11 cm of water, compared to the distribution of neat bottles is shown in Figure 38.

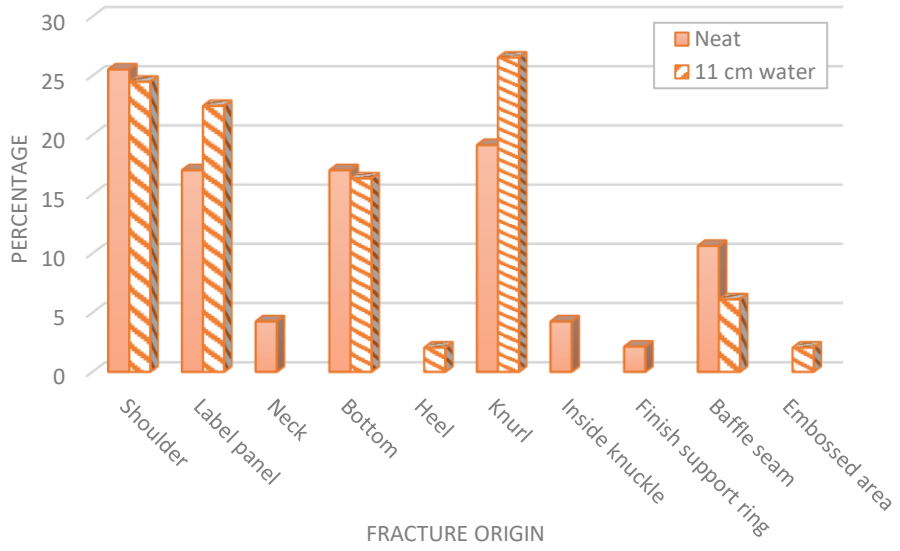

Figure 38: Distribution of fracture origin of bottle B, neat compared to frozen filled up to 11 cm

Most of the fractures still find their origin in the shoulder, the label panel, the bottom, or the knurl, which corresponds to the fracture origins of the neat bottles. Thus, no shift of fracture origin occurred by subjecting the bottles to internal pressure up to 11 cm in height.

4.2.2 Internal pressure resistance (IPR) during a Proof IPR test

During the *Proof IPR test* using the RPT 2, different values of pressure are applied to a series of 30 bottles per pressure value. The average of the measured IPR during the *Destruction IPR test* performed afterwards is shown in Table 10.

Table 10: IPR (bar) after Proof IPR test of internal pressure using RPT 2 – Bottle A

	Bottle A			
	Neat	*15.0 bar*	*20.0 bar*	*25.0 bar*
n	*100*	*30*	*30*	*29*
Average (bar)	**38.0**	**40.9**	**40.4**	**40.6**
Stdev	10.0	9.8	9.5	8.5
Min	17.3	22.0	18.3	28.5
Max	59.6	58.8	54.3	> 60.0
# not broken	/	/	/	1

During the *Proof IPR test* of 25.0 bar, one of the 30 bottles already broke at an internal pressure of 24.2 bar. This bottle could not undergo a *Destruction IPR test* after breakage. The series of 25.0 bar was therefore reduced to 29 bottles. Of the remaining 29 bottles, one did not break during the *Destruction IPR test* at a pressure below 60.0 bar, which is the limit of this test.

The average IPR values of the three series tested at a pressure of 15.0 bar, 20.0 bar, and 25.0 bar are respectively 40.9 bar, 40.4 bar, and 40.6 bar. There is no significant difference between the averages, as well as the averages do not differ significantly from the reference value of 38.0 bar for neat bottles, which shows that a *Proof IPR test* going up to 25.0 bar does not affect the strength of the glass bottles.

4.2.3 Topload pressure

A topload or vertical load will act on top of the bottles while capping the filled bottles during the packing process. If pallets are poorly or unevenly stacked during storage, the weight will no longer be distributed across all the bottles and a large weight may fall on a portion of the bottles. In these conditions, the bottles that carry the weight experience vertical pressure.

During a *Proof VLT test* using the Vertical Load Tester (VLT) in combination with the RPT 2, a topload pressure was applied to a series of bottles. One series only got loaded with 20,007 N once, while another series was loaded with 20,007 N eight times. The results of the *Destruction IPR test* after the application of topload, are shown in Table 11.

Table 11: IPR (bar) after applying topload pressure using VLT – Bottle A

	Bottle A		
	Neat	*1 x 20,007 N*	*8 x 20,007 N*
n	*100*	*30*	*30*
Average (bar)	**38.0**	**37.2**	**34.2**
Stdev	10.0	7.0	6.6
Min	17.3	28.7	20.1
Max	59.6	58.2	44.2

Returnable bottles aim for no breaks or functional defects at a load of 6002 N according to AB InBev's GTS [23]. While applying a topload of a greater force than 6002 N, no bottles broke during the load. After the application of the topload, a *Destruction IPR test* was applied. The series of bottles that were subjected to a load of 20,007 N once, appear not to be affected by the topload as the average IPR value of 37.2 bar does not differ significantly from the reference value of 38.0. By applying the same load several times, the strength of the bottles will decrease. After 8 times, the average IPR value appears to have dropped to 34.2. The t-test with 95% reliability results in a two-tail p-value of 0.02 meaning that the average IPR values of the neat bottles and the bottles that have been loaded with 20,007 N for eight times have a statistically significant difference. This difference is also reflected in the maximum measured IPR value, which dropped to 44.2 bar after the load.

The average IPR value of the series of bottles that were subjected to a topload of 20,007 N only once is not significantly different from the reference value. It is expected that there will be no shift in the distribution although this is not necessarily the case. Because of the significant difference in the average IPR value after eight times a topload of 20.007 N, a shift is expected for this distribution. The distributions of the different series of bottles tested for topload pressure are shown in Figure 39.

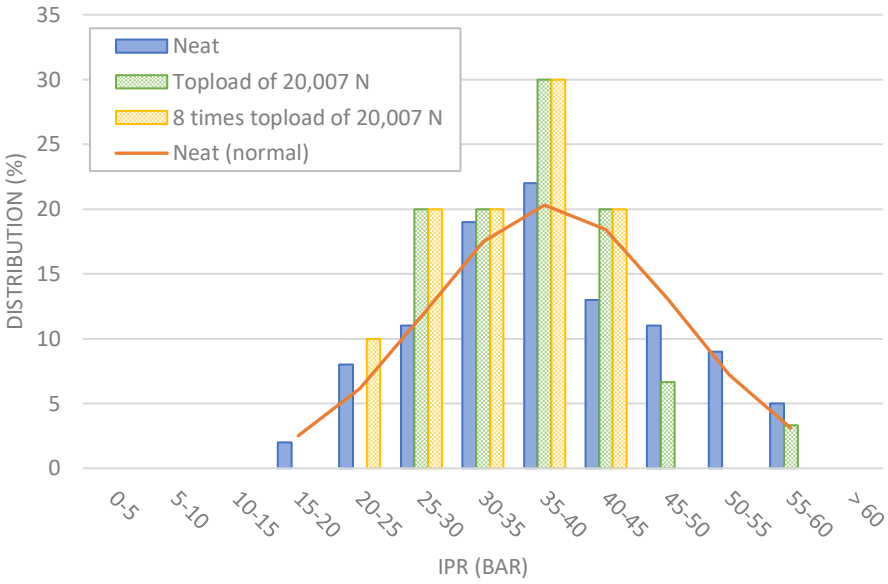

Figure 39: Distribution IPR (bar) after topload – Bottle A

Due to the fewer number of samples, the distribution does not appear to be completely similar. Nevertheless, the distribution remains within the same limits and the centre of the distribution falls similar to the one from the normal distribution of the reference samples. With a larger number of samples, the distribution would probably be the same.

As expected, for the bottles that were subjected to a topload of 20,007 N eight times a shift in the distribution has taken place relative to the normal distribution of the neat bottles. Not only has the entire distribution shifted to the left with a maximum measured IPR of 44.2 bar, but the shape of the distribution also appears to have changed. To properly analyse the shape, the number of tested bottles should have been higher than the 30 tested bottles. It could be estimated that the shape would be a right-tailed normal distribution.

4.2.4 Impact resistance

Impacts can occur at different times in the life cycle of a glass bottle, for example during transport or by the user of the bottle, at different locations at the glass plant, as well as during the labelling and packing of the bottles at the brewery. The effect of the impact depends on several factors, e.g. decreasing the striking velocity, stiffness, or mass of the glass results in a decrease in impact.

To find the most correct measuring method for the testing of the impact resistance of the bottles, both a manual and an automatic impact tester were used, where the impact was applied to the shoulder, at a height of 103 mm. The shoulder is most likely to be objected to impacts through the bottle's lifecycle as the area gets impacted most often by other bottles or surfaces whenever a bottle tilts. The angle to which the bottles were rotated after each stroke of impact was varied between 30°, 45°, and 120°. Table 12 shows the average maximum force with which the impact of the pendulum caused the bottle to break. The force is given in CPS or cm/s. Due to the limit of the test method at 320 CPS, not all tested bottles were broken, because these bottles have a higher impact resistance. For bottles whose effective impact resistance is therefore unknown, a value of 320 CPS is included in the calculation of the average impact resistance.

Table 12: Manual vs. automatic impact resistance (CPS) – Bottle A

	Bottle A			
	Manual	*Automatic*		
	Every 30°	*Every 30°*	*Every 45°*	*Every 120°*
n	*30*	*30*	*30*	*30*
Average (CPS)	**237**	**282**	**287**	**282**
Stdev	49	39	40	41
Min	140	190	150	200
Max	320	> 320	> 320	> 320
# not broken	/	7	12	9

All returnable bottles should be able to withstand one impact with an energy level of 89 CPS [23]. The lowest force at which one of the bottles broke is 140 CPS, which means all bottles fulfil the requirements.

The values obtained from the manual impact tester could depend on the operator performing the tests, as they have to hold the bottles themselves while impacting the pendulum. This could cause slight deviations of the results which could make the comparison with the automatic impact tester more difficult. But since the values of the manual impact tester are significantly lower, this factor will not play a major role in the comparison.

Both the averages and standard deviations of the results using the automatic impact tester are in fact higher than displayed in Table 12 as not all the 30 bottles tested came to a fracture. Some bottles can withstand a higher impact force than the limit of 320 CPS. The uncertainty of the actual standard deviation led to difficulty in the comparison of the manual and automatic impact testers. The automatic impact tester will be chosen as the better and most user-friendly option and will be used for further testing.

Between the results of the different angles, there are no significant differences measurable using this test method and this type of bottle, due to the high obtained values.

After choosing the automatic impact tester as the device that should be used for further testing, the effect of the number of strokes was analysed. While holding the bottle at its place so that multiple strokes of impact will hit the bottle at the exact same place at the shoulder and keeping the force of the impacts at a constant 100 CPS, the number of strokes was varied between 50, 100, and 150. After the application of impact, the bottles were conducted to a *Destruction IPR test*. The results of the measured IPR values are shown in Table 13.

Table 13: IPR (bar) after a different number of strokes at a force of 100 CPS – Bottle A

	Bottle A			
	Neat	*50 strokes*	*100 strokes*	*150 strokes*
n	*100*	*30*	*30*	*30*
Average (bar)	**38.0**	**38.4**	**31.6**	**35.8**
Stdev	10.0	9.2	11.3	9.4
Min	17.3	22.7	13.2	21.0
Max	59.6	56.5	53.4	55.8
Fracture origin at impact	N/A	0	8	7

The application of 100 strokes of a 100 CPS force impact seems to have the biggest impact on the strength of the bottles. The average IPR value of 31.6 bar shows a significant difference with a p-value below 0.004 as a result of a t-test with a 95% reliability from the reference value of 38.0 bar. It does appear that with 100 or more strokes, about one-fourth of the bottles have their fracture origin located at the site of the impact during the *Destruction IPR test*. The impact, therefore, appears to have caused sufficient damage to some of the bottles that the impact remains as the bottle's weakest point. For the other bottles, the impact did not cause enough damage and there were inherent flaws present that form an even weaker point in the bottle. In these bottles, the fracture will therefore not start at the impact site, but at a different location in the bottle.

Because the series of 50 and 150 strokes of impacts show no significant difference in average IPR compared to the reference value, the accuracy of the results of the series of 100 impacts is questioned. An increase in the bottle damage, leading to a decrease in the average IPR value would be expected with an increase in the number of strokes. Figure 40 shows the effect that the number of strokes has on the measured IPR values.

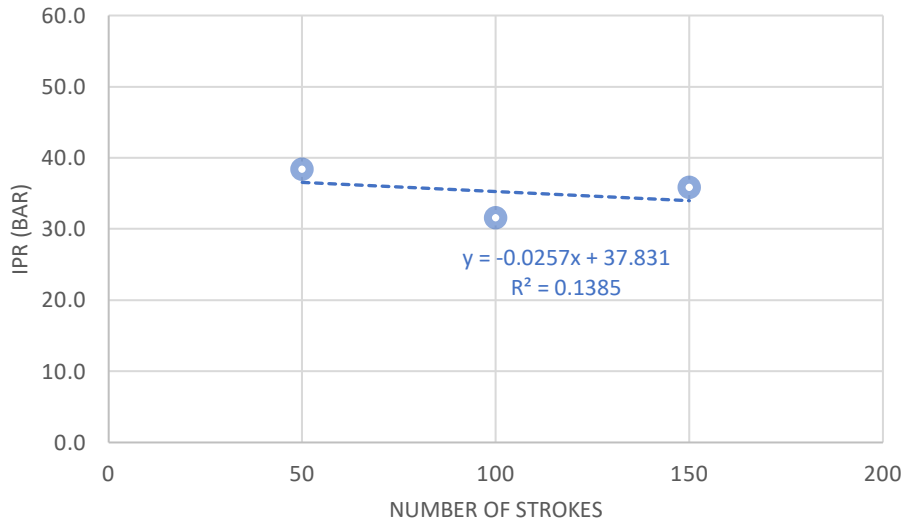

Figure 40: Influence of number of impact strokes on IPR of type A bottles

Based on the obtained results, it can be said that the effect of the number of strokes is not linear, which is confirmed by the R squared value. To confirm the effect, the series of 100 strokes should be repeated.

Besides the effect of the number of strokes, the effect of the force of the impact was investigated. The number of strokes was kept at a constant of 100 strokes, while the force was varied between 50 CPS, 100 CPS, and 150 CPS. The results from the *Destruction IPR test* conducted after the impacts were applied are shown in Table 14. The values of 100 CPS are the same values from 100 strokes in Table 13.

Table 14: IPR (bar) after 100 strokes at different forces – Bottle A

	Bottle A			
	Neat	*50 CPS*	*100 CPS*	*150 CPS*
n	*100*	*30*	*30*	*29*
Average (bar)	**38.0**	**35.1**	**31.6**	**33.3**
Stdev	10.0	8.3	11.3	11.2
Min	17.3	22.6	13.2	17.7
Max	59.6	> 60.0	53.4	> 60.0
# not broken	/	1	/	3
Fracture origin at impact	N/A	2	8	11

During the application of 100 strokes of 150 CPS one of the 30 bottles broke, leaving only 29 bottles to be conducted to the *Destruction IPR test*.

In the series of 50 CPS and 150 CPS, not all bottles broke during the *Destruction IPR test*, which means that the effective average IPR value is higher than displayed in Table 14.

The series of 100 CPS is the same as the series of 100 strokes in Table 13. The significant difference in average IPR value compared to the reference values again shows the lowest value of the series of 50 CPS, 100 CPS, and 150 CPS. From 100 strokes of impacts or 50 CPS, the force appears to be large enough to plastically deform the bottle and cause permanent damage, as several fractures have started at the impact site with each series of bottles. The number of fracture origins at the impact site during the *Destruction IPR test* appears to increase with increasing force, going from about one-fourth of the bottles at 100 strokes to more than one-third at 150 strokes. Despite the relationship between the average IPR values, this suggests that the effect of the impact would increase with increasing force. The effect of the force of the impacts is shown in Figure 41.

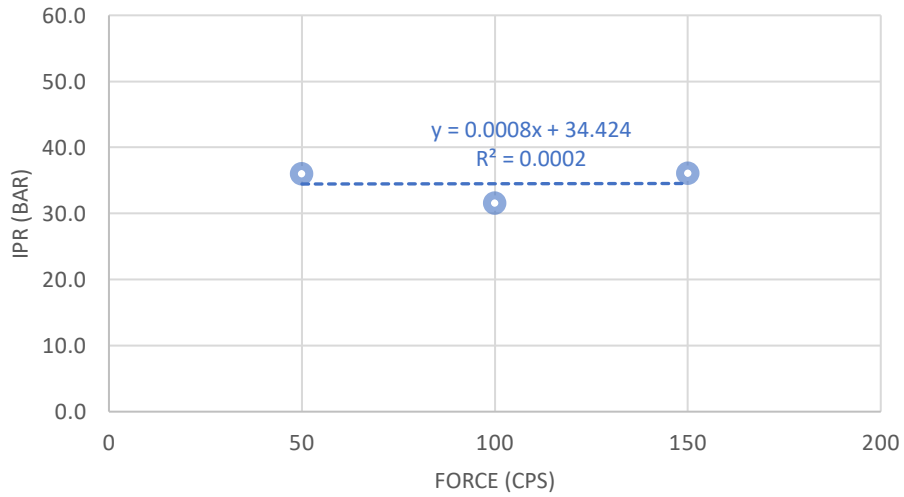

Figure 41: Influence of force of impacts on IPR of type A bottles

Based on Figure 41, the same conclusion could be drawn as the conclusion about the effect of the number of strokes. The effect of the force of the impact seems to be nonlinear, although the series of 100 strokes of 100 CPS should be retested to confirm.

Table 13 and Table 14 show the number of bottles where the fracture origin is located at the impact site. The three places that are affected by the impact were marked before the *Destruction IPR test* as

shown in Figure 24 to make it easier to confirm the location of the fracture origin. Whenever the fracture origin is located at one of the impact sites, it will look somewhat like the fracture origin pieces shown in Figure 42. These pieces are easy to recognize because of the markings.

Figure 42: Fracture after IPR (26.3 bar) with fracture origin located at impact site

Eight out of the 30 bottles tested for 100 strokes of impacts of 100 CPS had a fracture origin located at the impact site. Because it turns out these eight bottles were sufficiently affected by the impact to make this the weakest point in the bottle, the IPR values of these eight bottles can be examined. The comparison between the average IPR values of the total series with the average IPR values of the bottles with their origin at the impact site is shown in Table 15.

Table 15: Comparison of IPR with bottles with fracture origin at impact site – Bottle A

	Bottle A			
	Neat	*100 strokes of 100 CPS*		
n	*100*	*30*	*8*	*22*
Fracture origin			*At impact site*	*Somewhere else*
Average (bar)	**38.0**	**31.6**	**24.2**	**34.2**
Stdev	10.0	11.3	3.2	12.0
Min	17.3	13.2	18.4	13.2
Max	59.6	53.4	29.3	53.4

The average IPR value of the bottles with their fracture origin at the impact site of 24.2 bar has dropped significantly compared to the total series with an average IPR value of 31.6 bar. Whenever the impact had enough effect to make the impact site become the weakest point of the bottle, the IPR value will drop significantly compared to fractures due to inherent flaws. The low standard deviation of 3.2 bar shows that whenever the impact has become the weakest spot of the bottle and thus the site of fracture origin, the IPR value will always be about the same value of 24.2. In contrast, the bottles where the fracture origin is located at a different location in the bottle do have a large standard deviation, meaning that the fractures are a result of inherent flaws and are unaffected by the impact.

4.3 Effects of dynamic simulated stress

During the automatic filling and packing, refillable bottles experience friction with other bottles or surfaces. Friction mainly occurs during bottle transportation on the conveyer belt, where it occurs in combination with impact. A large proportion of bottles will exhibit scuffing after several cycles of refilling. The effect of friction was simulated in this study through a line simulation and scuffing simulation. After friction was applied to the bottles, they underwent a *Destruction IPR test* to compare the values obtained with the reference bottles. This comparison will show the effect of friction on the strength of the bottles.

4.3.1 Line simulation

After performing the line simulation, the bottles showed visible damage (Figure 43) due to friction with other bottles. At type A bottles, the damage is located at the shoulder of the bottle at a height of 103 mm measured from the bottom, where the chance of contact with other bottles is greatest. For type B bottles, the largest circumferences are located at 16 mm and 117 mm measured from the bottom, which are respectively the heel contact and the shoulder contact. The bottles will thus contact each other at these locations, causing scuffing at both heights.

Because there is a small gap between the 28 bottles in the line simulation, the contact will not only be broken and restored, but the bottles will also tilt and collide at an angle. The places on the bottles with the highest chances of friction are the same places where the impact will most likely occur. However, the damage is different per bottle, as not all bottles experience the same amount of friction and impact.

Figure 43: Scuffing after line simulation (5 min – 60 RPM – 40% slip)

Performing a 5-minute line simulation at 60 RPM should cause the same damage to the bottles that they would experience during transportation on a conveyer belt for multiple cycles in their lifetime [35].

To find out whether the line simulation only caused visual damage or also caused a reduction in the strength of the bottle, the bottles underwent a *Destruction IPR test*. Table 16 shows the results of the *Destruction IPR tests* on type A bottles at different rotation speeds of the moving belt. These tests were carried out on 28 filled bottles for 5 minutes with a slip rate of 40%. The slip rate causes the bottles to rotate 40% slower than the belt itself. Thus, at a setting of 30 RPM, the bottles will rotate at a speed of 18 RPM, while at a setting of 60 RPM, they will rotate at a speed of 36 RPM.

Table 16: IPR (bar) after 5 min line simulation at different speeds with 40% slip – Bottle A

	Bottle A			
	Neat	*30 RPM*	*45 RPM*	*60 RPM*
n	*100*	*28*	*28*	*28*
Average (bar)	**38.0**	**24.4**	**19.9**	**14.7**
Stdev	100	4.7	4.0	1.3
Min	17.3	16.3	13.1	12.3
Max	59.6	37.7	29.1	16.9

The series at different rotational speeds each obtained a significant reduction in average IPR value. The higher the rotation speed, the lower the measured IPR values appear to be. Because at a higher

rotation speed of the moving belt, the bottles will also rotate faster around their axis, there will be more friction between the bottles. The strength of the bottle-to-bottle impacts will also increase. In other words, more damage is observed in these bottles than at lower speeds.

To find out the linearity of this reducing effect on the strength of the bottle with increasing rotational speeds, the obtained results were plotted in Figure 44. The average IPR values are displayed relative to the rotation speeds.

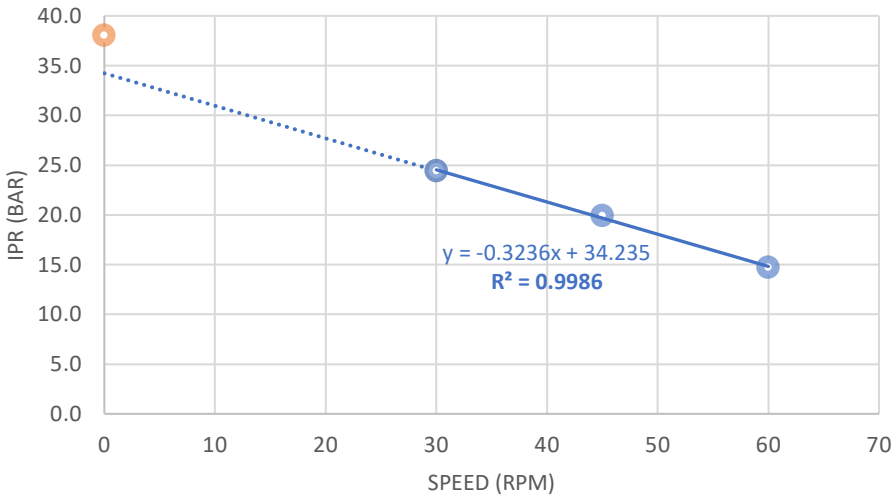

Figure 44: Influence of speed during line simulation on IPR of type A bottles

The high R-squared value of 0.9986 shows that the effect of rotational speed is indeed linear within the range of 30 RPM to 60 RPM. For rotation speeds that fall outside this range, it is not certain that the effect will remain linear over the entire curve.

In addition to the effect of speed, the effect of test time was also examined. The time of the simulation is varied between 2.5 minutes, 3.75 minutes, and 5.0 minutes. The speed of the belt remains constant at 60 RPM which causes the bottles to rotate at a speed of 36 RPM, due to the 40% slip rate. The average IPR values for the different series are shown in Table 17. The values of the 5-minute sequence are the same values from Table 16 of 60 RPM.

Table 17: IPR (bar) after line simulation at 60 RPM with 40% slip for different periods – Bottle A

	Bottle A			
	Neat	*2min 30s*	*3min 45s*	*5min 0s*
n	*100*	*28*	*28*	*28*
Average (bar)	**38.0**	**19.1**	**17.1**	**14.7**
Stdev	10.0	1.9	1.9	1.3
Min	17.3	15.4	12.9	12.3
Max	59.6	24.9	21.0	16.9

The effect of the duration time of the line simulation was plotted in Figure 45. The results of average IPR values are lined up in a straight line, which is confirmed by the R-squared value of 0.9971.

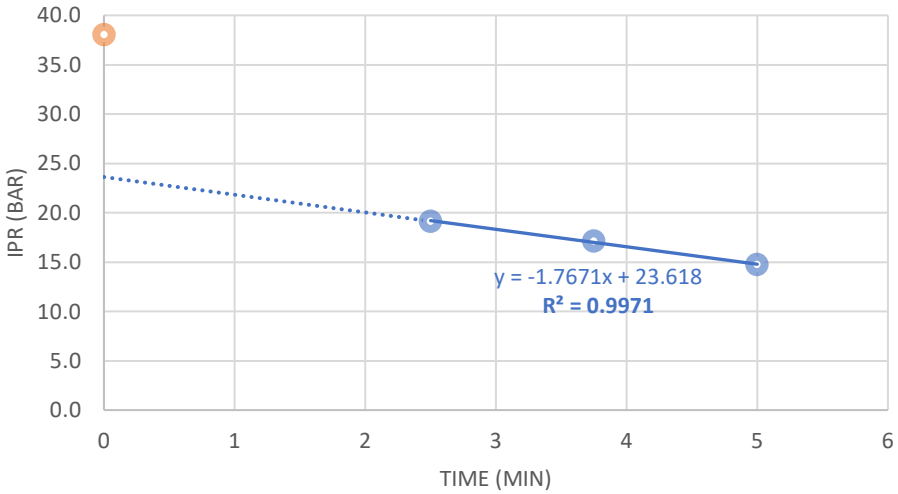

Figure 45: Influence of time during line simulation on IPR of type A bottles

The results of average IPR values are lined up in a straight line, which is confirmed by the R-squared value of 0.9971. In addition to the linear effect of the rotation speed, the effect of the duration time is also linear. However, the linearity can only be confirmed between the ranges of 2.5 minutes and 5.0 minutes.

Figure 46 shows an example of a fracture origin located at the height of the scuffing after the line simulation. This illustrates that the friction does not only cause visual damage but also increases the flaw severity in the location where the scuffing appeared. As a result of the flaws, the chances of breakage occurring at the scuffing area increase.

Figure 46: Fracture after IPR (12.0 bar) with fracture origin located at scuffing from line simulation

The series of the 5-minute line simulation with a rotation speed of 60 RPM and a slip rate of 40% were repeated. After this sequence, the bottles did not rest for 24 hours as in all previous tests and were used for a *Destruction IPR test* immediately after the line simulation. The average IPR values of both series with and without the 24-hour waiting period are shown in Table 18.

Table 18: IPR (bar) after 5-minute line simulation at 60 RPM with 40% slip rate with and without waiting period – Bottle A

	Bottle A		
	Neat	*5 min – 60 RPM – 40% slip*	
		24h waiting	*0h waiting*
n	*100*	*28*	*28*
Average (bar)	**38.0**	**14.7**	**14.2**
Stdev	10.0	1.3	1.4
Min	17.3	12.3	11.8
Max	59.6	16.9	16.4

The obtained values are remarkably similar. By means of a *Destruction IPR test*, no difference is observable between the 2 runs where there was and was not 24 hours of resting after performing the line simulation.

The same test was performed on the type B bottles to analyse the effect of duration time. The speed and slip rate were kept constant at 60 RPM and 40%, respectively. This time, a shorter duration time was chosen to start, as it is expected that the strength of the bottles will decrease faster on this type of bottle due to the larger circumference at the heel contact and shoulder contact. Both friction and impact will occur more rapidly at these locations. The results for the different line simulations of 30 seconds, 1 minute, 2 minutes, and 5 minutes are shown in Table 19. The obtained IPR values are compared with the reference values of type B bottles - Run 2 since these bottles come from the same production.

Table 19: IPR (bar) after line simulation at 60 RPM with 40% slip for different periods – Bottle B

	Bottle B				
	Neat	*30s*	*1min 0s*	*2min 0s*	*5min 0s*
n	*98*	*24*	*24*	*24*	*24*
Average (bar)	**27.2**	**18.2**	**16.5**	**16.4**	**16.1**
Stdev	7.6	2.4	2.9	2.0	1.3
Min	13.9	13	8.9	11.8	12.9
Max	47.0	22.6	20.9	20.0	18.1

From Table 19 can be seen that the strength of the bottles indeed decreases after the line simulation as a result of friction and impact. However, after 1 minute, the obtained IPR values and the strength of the bottles do not appear to decrease any further. To maintain a better understanding of the effect of the duration time, the obtained IPR values are plotted in Figure 47.

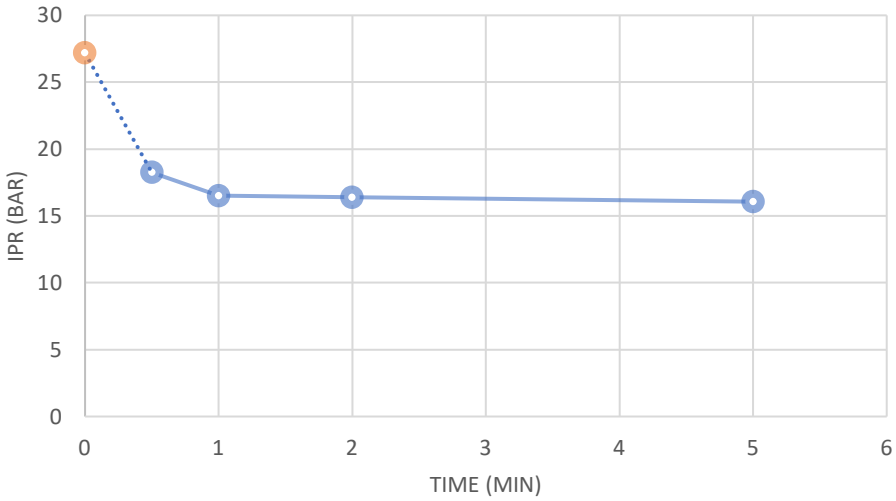

Figure 47: Influence of time during line simulation on IPR on type B bottles

Unlike type A bottles, duration time does not appear to have a linear effect on type B bottles. The strength of the bottles decreases significantly due to the line simulation up to 1-minute duration time. After 1 minute, a plateau is formed and the strength of the bottle remains constant. The strength of the bottle will not decrease further after more than 1 minute in the line simulator. The difference between the bottles is a result of the different shapes, with the circumference at the heel contact and shoulder contact of bottle B being greater than at the rest of the bottle (Figure 13, paragraph 3.1). The slightly protruding heel contact and shoulder contact ensure more contact between the bottles.

4.3.2 Scuffing simulation

After a scuffing simulation of 10 minutes, most bottles show slightly visible damage (Figure 48) at the circumference where scuffing has occurred at a height of 65 mm measured from the bottom, which is located in the label panel and not on the shoulder as after the line simulation. In a small number of bottles, thin white lines (Figure 49), resembling scratches, are present in the band of scuffing. Other than that, there is no visual damage to the bottles.

Figure 48: Slightly visible damage after scuffing simulation

Figure 49: Thin white scratches after scuffing simulation

After a series of 30 bottles had been scuffed for 10 minutes, a *Destruction IPR test* was performed from which the average value for the maximum internal pressure that the bottles achieved was obtained and shown in Table 20.

Table 20: IPR (bar) after 10min scuffing simulation with a rotation speed difference of 40 RPM and a pressure of 2 bar – Bottle A

	Bottle A	
	Neat	*10min*
n	*100*	*30*
Average (bar)	**38.0**	**37.0**
Stdev	10.0	9.3
Min	17.3	19.6
Max	59.6	59.0
Fracture origin at scuffing	N/A	9

With an average IPR value of 37.0, there is no significant difference compared to the neat bottles. Whenever the damage as a result of scuffing is only slightly visible, the strength of the bottles is not reduced. However, in 30% of the bottles, the fracture origin was located at the place where friction had taken place (Figure 50). The damage as a result of scuffing is not significantly larger than the damage that was already present on the bottles before the scuffing simulation.

Figure 50: Fracture after IPR (30.5 bar) with fracture origin located at scuffing area after scuffing simulation

Nine out of the 30 bottles scuffed for 10 minutes at a rotation speed difference of 40 RPM and a pressure of 2 bar, with one of the bottles tilted at a 45° angle, had their fracture origin located at the area where friction had occurred. To find out if scuffing does affect the IPR values besides the effect it has on the distribution of the location of fracture origins, Table 21 compares the IPR values of fractures at the scuffing area with the total series of the scuffing simulation.

Table 21: Comparison of IPR with bottles with fracture origin at scuffing area – Bottle A

	Bottle A		
	Neat	*10 min scuffing simulation*	
n	*100*	*30*	*9*
Fracture origin			*At scuffing area*
Average (bar)	**38.0**	**37.0**	**36.3**
Stdev	10.0	9.3	8.7
Min	17.3	19.6	19.6
Max	59.6	59.0	45.6

Even though the average IPR value of 36.3 bar does not appear to be significantly different from the reference value, the maximum measured IPR value of 45.6 bar is quite a bit lower compared to 59.6 bar at the neat bottles. It can be concluded that for bottles where scuffing is the cause of fracture, the measured IPR value will not exceed 45.6 bar, although further research is needed on a larger number of bottles to say this with certainty.

While scuffing the bottles for the Design of Experiments (DoE), 15% of the bottles developed a thicker white line over the entire scuffing circumference. From the moment one of the bottles, as a result of a non-homogeneous coating, falters and no longer achieves the set rotation speed, a white line emerges. This line becomes larger and brighter as the bottle continues to scuff. The bottles with white lines were not used for the Design of Experiments and were kept aside for individual testing.

The bottles that would have been used for Run 1 through Run 4 of the DoE were scuffed for 10 minutes, while the bottles that were meant for Run 5 through Run 8 have been through 15 minutes of scuffing at the same settings.

Before the *Destruction IPR test* the bottles were placed in order of visible scuffing severity based on the even-numbered bottle, that stayed upright during the scuffing, per scuffed pair (Figure 51 and Figure 52), and were tested in that order.

Figure 51: Visible scuffing after 10 minutes ranked from most to least severe

Figure 52: Visible scuffing after 15 minutes ranked from most to least severe

Table 22 shows the average IPR values of the scuffed bottles with visual damage compared to the reference value of the neat bottles.

Table 22: IPR (bar) after scuffing simulation causing visible scuffing – Bottle A

	Bottle A		
	Neat	*10min*	*15min*
n	*100*	*18*	*26*
Average (bar)	**38.0**	**21.0**	**22.3**
Stdev	10.0	3.9	4.6
Min	17.3	14.7	15.2
Max	59.6	28.0	30.4
Fracture origin at scuffing	N/A	18	21

From Table 22 it can be deduced that the bottles that have suffered very visible scuffing as a result of friction do experience a significant reduction in strength as the average IPR values have decreased to 21.0 bar and 22.3 bar for respectively 10 minutes and 15 minutes of scuffing. In most of the bottles where there was visible damage due to the scuffing, this circumference encompasses the weakest point of the bottle, as 18 out of 18 and 21 out of 26 bottles had their fracture origin located at the scuffing area (Figure 53). The five bottles from the 15 minutes of scuffing where the fracture origin is located somewhere else in the bottle were all bottles that had been tilted at a 45° angle.

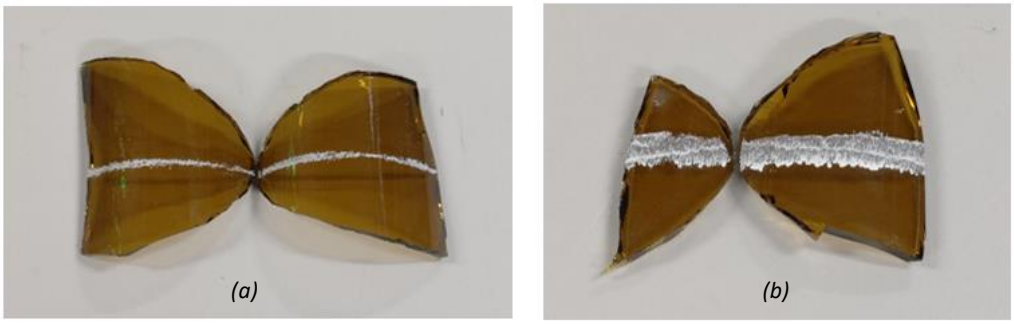

Figure 53: Fracture after IPR (17.0 bar) (a) and IPR (27.1 bar) (b) with fracture origin located at scuffing area after scuffing simulation

The damage on the tilted bottles, therefore, appears to have less influence than the damage on the bottle that remained upright. This assumption is confirmed by comparing the visual damage on the tilted bottle on the left and the upright bottle on the right (Figure 54).

Figure 54: Pair of scuffed bottles with visual damage

The scuffing on the tilted bottles seems to be spread over a larger surface than the damage on the upright bottle. This is because one of the bottles continuously adjusts its position so that the pressure that the bottles exert on each other remains constant. As a result, the damage on the tilted bottle is also slightly higher than on the upright bottle.

Figure 55 shows the distribution of the IPR values per bottle to compare the tilted bottles with the upright bottles.

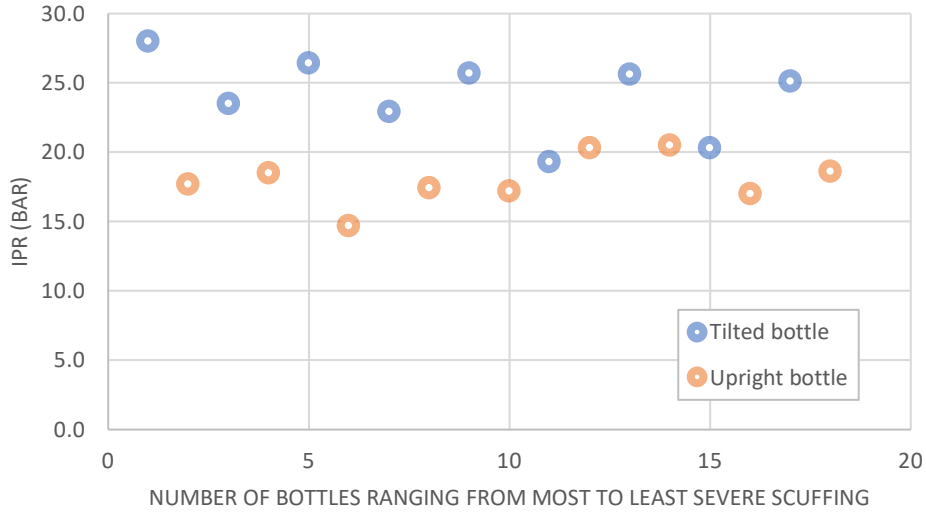

Figure 55: Distribution of IPR (bar) of tilted and upright bottles after scuffing simulation – Bottle A

Figure 55 confirms once again that the strength of the tilted bottles has decreased less than the upright bottles because the scuffing is spread over a bigger surface.

The bottles that are displayed on the left-hand side of the graph are the bottles that suffered the most severe scuffing. The bottles on the right-hand side only showed a thin withe line as a result of the scuffing. Nevertheless, no correlation can be seen between the results going from left to right. That is, the severity of the scuffing does not affect the measured IPR values and hence the strength of the bottle. From the moment visible damage has occurred, the strength drops significantly, but the size of the damage has no influence.

4.4 Combination of selected effects (DoE)

To get a first idea of the size of the individual effects of friction, topload pressure, and impact and the interactions between these effects, a first Design of Experiments was done. Each combination of factors, except friction individually and friction in combination with topload pressure, was applied, followed by a *Destruction IPR test*. The applied factors are shown in Table 23 per run together with the average IPR values obtained.

Table 23: IPR (bar) of different combinations of friction, topload, and impact – Bottle A

	Bottle A				
	Run 1	*Run 2*	*Run 3*	*Run 4*	*Run 5*
n	*30*	*30*	*28*	*30*	*28*
Friction			*x*		*x*
Topload	*x*			*x*	*x*
Impact		*x*	*x*	*x*	*x*
Average (bar)	**37.2**	**31.6**	**14.7**	**36.5**	**16.4**
Stdev	7.0	11.3	1.3	9.0	2.2
Min	28.7	28.7	12.3	22.5	12.9
Max	58.2	58.2	16.9	> 60.0	22.2

The results of Run 2 are taken from previous tests where 100 strokes of 100 CPS impacts were applied. It was previously indicated that the reliability of these results was questioned and that the test should be repeated to be sure of the conclusion.

From Table 23 it appears that applying a top load pressure does not affect the strength of the bottle at all. This follows from the results of Run 1 but is also confirmed by the difference in the results of Run 3 and Run 5. The line simulation of Run 3, where friction and impact are applied, causes a significant decrease in the average IPR value. If a top load is also applied to the same bottles, as in Run 5, the average IPR value does not drop any further.

In Table 24, the reduction in average IPR value compared to the reference value of 38.0 bar of the neat bottles is ranked per factor or combination of factors.

Table 24: Percentage of reduction in IPR – Bottle A

	Run	*Average*	*Reduction*	***Percentage***
Topload	*1*	*36.4*	*1.6*	***4%***
Impact	*2*	*31.6**	*6.4*	***17%***
Friction + impact	*3*	*14.7*	*23.3*	***61%***
Friction**				**44%**
Topload + impact	4	36.5	1.5	**4%**
Friction + topload + impact	5	16.4	21.6	**57%**
Friction + topload**				**40%**

**Test results to be confirmed*
***Estimations based on Run 2 and Run 3 or Run 5*

From Table 24 it can be concluded that the line simulation is the only one that causes a significant decrease in average IPR value of 61% at Run 3 and 57% at Run 5. Whether that effect mainly comes from the friction or from the impact the bottles experience during the line simulation can only be estimated using the results of Run 2, where only impact was applied. It is then assumed that the impact that occurs during the line simulation is equal to the impact of Run 2, which was 100 impact strokes of 100 CPS. The results for friction and friction in combination with top load are therefore only an estimate based on the other results. The percentages are ranked in Figure 56 for a clear overview of the effects.

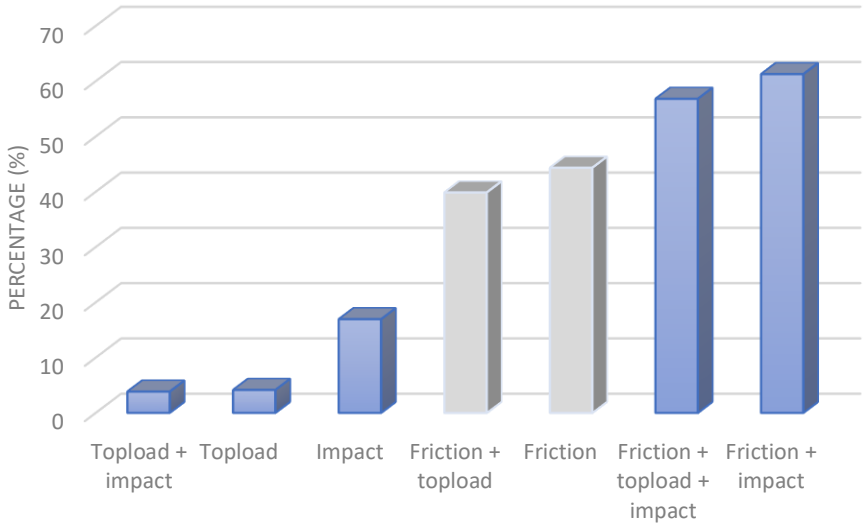

Figure 56: Percentage of reduction in IPR – Bottle A

The combination of friction with impact appears to cause the greatest reduction in average IPR value. Of the individual effects, friction would cause the most damage to the glass bottles, although these results are only an estimate. Friction is followed by impact, while topload pressure does not influence the strength of the bottle.

Since the results of the first DoE attempt can only provide an estimate of the effects of each factor, a second DoE was performed. This time a full DoE, where both a high and a low setting were chosen for each factor. All possible combinations of high and low values were tested, as shown in Table 25.

Table 25: Design of Experiments – Bottle A

	Bottle A							
	Run 1	*Run 2*	*Run 3*	*Run 4*	*Run 5*	*Run 6*	*Run 7*	*Run 8*
n	*30*	*30*	*30*	*30*	*30*	*30*	*30*	*30*
Friction	*-1*	*-1*	*-1*	*-1*	*+1*	*+1*	*+1*	*+1*
Topload	*-1*	*-1*	*+1*	*+1*	*-1*	*-1*	*+1*	*+1*
Impact	*-1*	*+1*	*-1*	*+1*	*-1*	*+1*	*-1*	*+1*
Average (bar)	**36.1**	**34.9**	**35.5**	**35.6**	**32.9**	**35.0**	**34.5**	**35.9**
Stdev	8.6	7.1	8.2	8.3	5.8	8.9	7.7	7.3
Min	19.1	21.0	22.3	19.7	24.5	15.9	14.1	21.3
Max	> 60.0	48.6	48.7	52.3	45.9	49.9	51.0	53.2
Fracture origin at scuffing	6	14	12	9	11	8	7	10

There appear to be no clear differences between the results of the different runs. This is probably because the settings for applying friction, topload, and impact have been chosen as close as possible to what is expected by the standard. These setting values are too low to cause sufficient damage to the bottle and to deduce the effects and interactions from the results. This means that the bottles certainly meet the standards for returnable bottles.

Based on the results in Table 25, the effect of friction, topload pressure, and impact cannot be observed, so the interactions between the three factors cannot be analysed either. In order to get a clear picture of the effects and interactions, the chosen settings must be chosen differently. For this

reason, it is not useful to conduct further tests with these settings to verify the effect of the order in which friction, topload pressure, and impact are applied.

From Table 25 it appears that in an average of 10 of the 30 bottles, the fracture origin is located at the site of the scuffing. In these bottles, the circumference of the scuffing has become the weakest spot, but this does not cause a decrease in IPR values, as was shown earlier. None of the bottles had a fracture origin located at the impact site. The impact site, on bottles that have been objected to the combination of friction, topload, and impact, no longer appears to be the point with the greatest chance of fracture.

5. Conclusion

The main objective of this study was to quantify the relationship between the individual and combined effects of friction, impact, and pressure on the strength of selected types of glass bottles to predict the quality of reusability in a simulation process.

First, the internal pressure resistance (IPR) the bottles can withstand was measured for both type A and B bottles through a *Destruction IPR test*. Type A bottles were found to obtain an average IPR value of 38.0 bar ± 10.0 bar. The average IPR values of the two deliveries of type B bottles were found to be significantly different. This may be a result of a change or error in the process or mold used. Nevertheless, both average IPR values of type B bottles of 42.2 bar and 27.2 bar meet the quality requirement of an average IPR value greater than 25.0 bar. These values were used as reference values further in the study.

During these *Destruction IPR tests*, the locations of the fracture origin were checked and the distribution was analyzed by area of the bottle. For bottle A, fracture origins were found to be nicely distributed over the surface of the bottle. For the fractures of bottles B, more fracture origins relative to the surface were located in the bottom, knurl, and baffle seam, which may be a result of imperfection in the mold or poor cooling.

After applying internal pressure due to the expansion of frozen water, the shoulder of the bottle was found to be the least resistant to internal pressure. Bottles A which were filled to 9 cm or lower and bottles B which were filled to 11 cm or lower could withstand the internal pressure well, and no fractures were found to occur in these bottles. After performing a *Destruction IPR test* on the bottles that could withstand the frozen water, a slight but not significant decrease in average IPR value was found when compared to the reference values. Furthermore, the distribution of fracture origins did not appear to have changed compared to the neat bottles.

Performing a *Proof IPR test* with a set pressure of 15.0 bar, 20.0 bar, or 25.0 bar on type A bottles was found to not affect the subsequently measured IPR values by a *Destruction IPR test*.

Since the quality requirements state that no fractures or functional defects should occur at a topload of 6002 N, a series of type A bottles was subjected once to a topload of 20,007 N, which is the test limit of the device, to verify the force at which fractures occur. After all bottles achieved a topload of 20,007 N without fractures occurring, they were subjected to a *Destruction IPR test*. The average IPR value was found to be not significantly different from the reference value. Another series of type A bottles were subjected to the same topload eight times and this time the average IPR value dropped to 34.2, which compared to the neat bottles represents a significant difference.

While testing the impact resistance of the Type A bottles with different methods, the lowest measured value was found to be 140 CPS, which lies above the quality requirement of 89 CPS. To say with certainty that 100 strokes of impacts of 100 CPS have a significant effect on the measured IPR values of the bottles, the test would have to be repeated. Performing 50 or 150 strokes of 100 CPS and 100 strokes of 50 CPS or 150 CPS does not cause a decrease in average IPR values. Nevertheless, it appears that from 100 strokes or impacts of 100 CPS going up the obtained defect is sufficiently large so that in about one-fourth of the bottles the fracture origin is located at the impact site.

After performing a line simulation on type A bottles, scuffing was found to have occurred at the shoulder of the bottle. On type B bottles, the line simulation affected both the heel and the shoulder since the circumference is greatest at these locations. As a result of both impact and friction occurring

during the line simulation, a sharp drop in average IPR value occurred. A series of type A bottles subjected to a 5-minute line simulation with a 60 RPM rotation speed and 40% slip obtained an average IPR value of 14.7 bar. Type B bottles obtained an average IPR value of 16.1 bar after the same line simulation. Both the rotation speed and duration time have a linear effect on the reduction in IPR. Future research could examine the effect of the slip rate during the line simulation.

From the moment scuffing occurs on the type A bottles due to a non-homogenous coating layer during the scuffing simulation with a pressure of 2 bar and a rotational speed differential of 40 RPM, the average IPR value decreases to 21.0 bar and 22.3 bar for 10 minutes and 15 minutes of scuffing simulation, respectively. Thereby, the fracture origin will almost always be located at the circumference where scuffing has occurred. To complete the optimization of this test method, the effect of the rotation speed, pressure, and angle between the bottles could be examined.

Based on the combination of factors, it can be concluded that friction, as a result of the line simulation or scuffing simulation, causes the greatest reduction in IPR values and has the greatest influence on the strength of the bottle. To complete the simulation, the test of 100 strokes or impacts at 100 CPS should be performed again to be able to say with certainty that impact influences the measured IPR values. Pressure, in the form of internal pressure and topload pressure, does not appear to cause a significant drop in IPR values. It can therefore be concluded that the amount of pressure applied in the tests carried out does not influence the strength of the bottle. So, the simulation should not include any kind of pressure to make the simulation as fast and user-friendly as possible.

After applying the combination of friction, topload pressure, and impact, it appears that no interactions occur between the three factors and that they do not have an influence on each other. From these results, it can be concluded that the order in which the three factors are applied will not affect the strength of the bottles.

After having to search for the fracture origin several times, both to find out the distribution of fracture origins in the neat bottles and during the search for fracture origins after impact and/or friction, sufficient experience has been gained in fractography. It is now much easier to find a fracture origin because the fracture patterns are known and lead to the point of origin.

Reference list

[1] "AB InBev," Anheuser-Busch InBev, 2023. [Online]. Available: https://ab-inbev.be/. [Accessed 12 April 2023].

[2] "O-I Glass Catalog," O-I, 2023. [Online]. Available: https://glass-catalog.com/eu-en/catalog#cat-beer=true&page=1-60&returnable=1. [Accessed 12 April 2023].

[3] "Ab InBev ontwikkelt lichtere bierfles," Verpakkingsmanagement, 8 Juni 2021. [Online]. Available: https://www.verpakkingsmanagement.nl/techniek/nieuws/ab-inbev-ontwikkelt-lichtere-bierfles. [Accessed 12 April 2023].

[4] "'Lichtste bierfles ter wereld' ontwikkeld bij AB InBev," Packaging magazine, 12 Juni 2021. [Online]. Available: https://packagingmagazine.be/lichtste-bierfles-ter-wereld-ontwikkeld-bij-ab-inbev/. [Accessed 12 April 2023].

[5] "Circular packaging - Driving Sustainable Packaging," AB InBev, 2021. [Online]. Available: https://www.ab-inbev.com/sustainability/circular-packaging/. [Accessed 7 April 2023].

[6] "ISO 18603:2013(en) Packaging and the environment — Reuse," ISO, 2012. [Online]. Available: https://www.iso.org/obp/ui/#iso:std:iso:18603:ed-1:v1:en. [Accessed 14 April 2023].

[7] R. Stefanini, G. Borghesi, A. Ronzano and G. Vignal, "Plastic or glass: a new environmental assessment with a marine litter indicator for the comparison of pasteurized milk bottles," in *The International Journal of Life Cycle Assessment*, vol. 26, Springer, 2021, p. 767–784. https://doi.org/10.1007/s11367-020-01804-x

[8] "Milieu Impact AB InBev België," 2022. [Online]. Available: https://ab-inbev.be/sites/default/files/2022-09/AB%20Inbev%20Impac%20Report%202022%20low-res.pdf. [Accessed 12 April 2023].

[9] Ellen Macarthur Foundation, "What is a circular economy?," Ellen Macarthur Foundation, [Online]. Available: https://ellenmacarthurfoundation.org/topics/circular-economy-introduction/overview#principles. [Accessed 19 July 2023].

[10] Ellen Macarthur Foundation, "Circulate products and materials," Ellen Macarthur Foundation, [Online]. Available: https://ellenmacarthurfoundation.org/circulate-products-and-materials. [Accessed 19 July 2023].

[11] Ellen Macarthur Foundation, "The butterfly diagram: visualising the circular economy," Ellen Macarthur Foundation, [Online]. Available: https://ellenmacarthurfoundation.org/circular-economy-diagram. [Accessed 19 July 2023].

[12] Ellen Macarthur Foundation, "Reusable packaging business models," Ellen Macarthur Foundation, [Online]. Available: https://ellenmacarthurfoundation.org/reusable-packaging-business-models. [Accessed 19 July 2023].

[13] K. Van Acker, K. Allacker, K. Bachus, K. Biedenkopf, K. Binnemans, W. Dewulf, M. Dubois, J. Duflou, J. Eyckmans, P. Muchez, L. Pandelaers, G. Van Calster, T. Van Gerven and L. Vranken, "Circular economy," Leuven, 2016.

[14] Ellen Macarthur Foundation, "About us - What we do," Ellen Macarthur Foundation, [Online]. Available: https://ellenmacarthurfoundation.org/about-us/what-we-do#:~:text=We%20are%20a%20non%2Dprofit,benefits%20of%20a%20circular%20economy. [Accessed 2023 July 2023].

[15] M. Boonen, "AB InBev - Environmental, Social & Governance Report," AB InBev, Antwerp, Belgium, 2022.

[16] K. Lambers, "Why Does Beer Taste Better in Glass?," O-I, 7 November 2022. [Online]. Available: https://www.o-i.com/news/why-does-beer-taste-better-in-glass/#:~:text=Taste%20preservation%20and%20quality%20are,effective%20barrier%20against%20external%20influences.. [Accessed 17 April 2023].

[17] T. M. Mata and C. A. Costa, "Life Cycle Assessment of Different Reuse Percentages for Glass Beer Bottles," in *International Journal of Life Cycle Assessment*, vol. 6, Porto, Springer, 2001, p. 307–319.
https://doi.org/10.1007/BF02978793

[18] K. Van Doorsselaer and F. Lox, "Estimation of the Energy Needs in Life Cycle Analysis of One-way and Returnable Glass Packaging," in *Packaging Technology and Science*, vol. 12, Brussels, John Wiley & Sons, 1999, pp. 235-239.
https://doi.org/10.1002/(SICI)1099-1522(199909/10)12:5<235::AID-PTS474>3.0.CO;2-W

[19] C. Tua, M. Grosso and L. Rigamonti, "Reusing glass bottles in Italy: A life cycle assessment evaluation," in *Procedia CIRP*, vol. 90, Milano, Elsevier, 2020, pp. 192-197.
https://doi.org/10.1016/j.procir.2020.01.094

[20] J. Cleary, "Life cycle assessments of wine and spirit packaging at the product and the municipal scale: a Toronto, Canada case study," in *Journal of Cleaner Production*, Toronto, Elsevier, 2013, pp. 143-151.
https://doi.org/10.1016/j.jclepro.2013.01.009

[21] D. R. Morgan, D. Styles and E. T. Lane, "Packaging choice and coordinated distribution logistics to reduce the environmental footprint of small-scale beer value chains," in *Journal of Environmental Management*, vol. 307, Elsevier, 2022.
https://doi.org/10.1016/j.jenvman.2022.114591

[22] G. De Feo and C. Ferrara, "Comparative life cycle assessment of alternative systems for wine packaging in Italy," in *Journal of Cleaner Production*, vol. 259, Fisciano, Italy, Elsevier, 2020.
https://doi.org/10.1016/j.jclepro.2020.120888

[23] AB InBev Group, "Global Packaging General Technical Specifications (GTS) for Glass Bottles," 2021.

[24] “General data sheets - Tolerances, specifications and control procedures, general characteristics,” Cetie - Free voluntary standards for Glass and PET packaging, 11 January 2023. [Online]. Available: https://www.cetie.org/en/general-data-sheets-dt_123.html. [Accessed 17 August 2023].

[25] D. Cannon, C. Musso, J. Williams and T. Eagar, “Analysis of Brittle Fracture of Soda Glass Bottles under Hydrostatic Pressure,” in *Journal of Failure Analysis and Prevention*, vol. 4, ProQuest, 2004, p. pages72–77. https://doi.org/10.1361/15477020420800

[26] N. I. Minko and V. M. Nartsev, “Factors Affecting the Strength of the Glass (Review),” in *Middle East Journal of Scientific Research*, vol. 18, Russia, IDOSI Publications, 2013, pp. 1616-1624. 10.5829/idosi.mejsr.2013.18.11.70117

[27] G. D. Quinn, Fractography of Ceramics and Glasses, U.S.: National Institute of Standards and Technology, 2016.

[28] O-I, “How to read a glass bottle,” O-I, [Online]. Available: https://www.o-i.com/our-story/how-to-read-a-glass-bottle/. [Accessed 2 June 2023].

[29] Ardagh Group, “30000497 330ml flint glass Longneck returnable beer bottle,” Ardagh Group, 2023. [Online]. Available: https://www.ardaghproducts.com/product-specification/longneck-mw-330-c30-26c2. [Accessed 19 July 2023].

[30] Agr International, Inc., “Ramp Pressure Tester 2X,” December 2016. [Online]. Available: https://www.agrintl.com/wp-content/uploads/2016/12/RPT2X1216_NS-1.pdf. [Accessed 12 April 2023].

[31] AGR International, Inc., “Ramp Pressure Tester 2 - Operation Manual,” Butler, Pennsylvania, 2003.

[32] Agr International, Inc., “Vertical Load Strength Measurement,” 2016. [Online]. Available: https://www.agrintl.com/wp-content/uploads/2016/03/VLT0915NS.pdf. [Accessed 12 April 2023].

[33] AGR International, Inc. , “Vertical Load Tester - Operation Manual,” Butler, Pennsylvania, 1996.

[34] Agr International, Inc., “Impact Tester - Tests the Impact, Dent, and Puncture Resistance of Containers,” 2016. [Online]. Available: https://www.agrintl.com/wp-content/uploads/2016/03/IT_2_redesign.pdf. [Accessed 14 April 2023].

[35] Agr International, Inc., “Line Simulator - Filling Line Abrasion Simulation,” 2016. [Online]. Available: https://www.agrintl.com/wp-content/uploads/2016/03/Line_Simulator_redesign.pdf. [Accessed 14 April 2023].